2012

ROLE OF TYROSYL-DNA PHOSPHODIESTERASE (TDP 1) ON REPAIR OF 3'-PHOSPHOGLYCOLATE (3'- PG) TERMINATED DNA DOUBLE-STRAND BREAKS (DSBS) AND IN RESPONSE TO OXIDATIVE STRESS

Tong Zhou
Virginia Commonwealth University

ROLE OF TYROSYL-DNA PHOSPHODIESTERASE (TDP 1) ON REPAIR OF 3′-PHOSPHOGLYCOLATE (3′- PG) TERMINATED DNA DOUBLE-STRAND BREAKS (DSBS) AND IN RESPONSE TO OXIDATIVE STRESS

A thesis submitted in partial fulfillment of the requirements for the degree of Master of Science at Virginia Commonwealth University

By

Tong Zhou

B.M. in Clinical Medicine, China Medical University, 1989

Director: Lawrence F. Povirk, Professor, Department of Pharmacology and Toxicology

Virginia Commonwealth University

Richmond, Virginia

December, 2012

ACKNOWLEDGEMENT

First, I would like to express my sincere and deepest gratitude for Dr. Lawrence F. Povirk, who has been an excellent mentor and a phenomenal advisor. I can't thank him enough for all the guidance, support and incredible patience that I received over the years and without which this thesis work would not have been possible. It has been a great personal experience working in his laboratory. I still retained some of the notes that he wrote to me so that I knew how to start daily work when I first joined his laboratory. Dr. Povirk is a great scientist with a pleasing and noble personality. I consider myself lucky for getting an opportunity to interact with him and learn a lot about the field of study. I would also like to thank the members of my committee, Dr. Aylin Marz and Dr. Joseph Ritter for giving me valuable suggestions, encouragement, and guidance throughout my thesis work.

I would like to thank all of my lab members for their consistent help and support, especially Dr. Konstantin Akopiants and Dr. Susovan Mohapatra for all the great time we have had, and for all the guidance, career advice and most of all for being such great friends. I would also like to thank Vijay Menon who is a Ph.D student in the same program, thank him for helping select appropriate courses and helping me with some procedures in my experiments. I would also like to thank Mohammed Al Mohaini for helping me edit my thesis.

I am really grateful of the core lab manager Ms. Frances White and Julie Farnsworth for their immense help and support with my confocal microscope and flow cytometric experiments. I would also like to thank Dr. Pick-Sun Lin for teaching me the technique of metaphase spreads and preparation of micronuclei slides.

I would also like to thank my wonderful husband Ruizhe Zhou and my lovely children Kevin and Eric for their love and support. My husband took over all the housework during my preparation of thesis and final defense. Kevin supported mom's study by doing his study and managing himself perfectly in his college, and Eric supported by not bothering me a lot and doing extremely well in his elementary school.

Finally, I would like to thank my parents, Shitai Zhou and Xichun Li for their love and support. They have always encouraged me in my decisions and have made immense sacrifices so as to make my life better. They truly are the foundations of my well-being and will continue to be. I would like to thank my sisters for helping me take care of my parents.

TABLE OF CONTENT

LIST OF FIGURES

LIST OF ABBREVIATIONS

Å	angstrom
AOA	ataxia with oculomotor apraxia
AP	apurinic/apyrimidinic
APE1	apurinic/apyrimidinic endonuclease
ATM	Ataxia Telangiectasia Mutated
ATP	Adenosine triphosphate
ATR	Ataxia Telangiectasia and RAD3-related
BASC	BRCA1-associated genome surveillance complex
BER	base excision repair
BLM	Bloom syndrome, RecQ helicase-like
53BP1	p53 binding protein 1
BRCA1 (2)	breast cancer type 1 (2) susceptibility protein
Ca	Calcium
CDK	cyclin-dependent kinase
CHO	chinese hamster ovary cell
CKI	cyclin-dependent kinase inhibitor protein
CPT	camptothecin
DAPI	4', 6-diamino-2-phenylindole
DMSO	dimethyl sulfoxide
DNA	deoxyribonucleic acid
DNA-PK	DNA-dependent protein kinase
DNA-PKcs	DNA-dependent protein kinase catalytic subunit
DSBs	double-strand breaks
H493R	histidine 493 residue
HKD motifs	histidine-lysine domain motifs

Hr	Hour(s)
γ-H2AX	phosphorylated H2AX
H_2O_2	hydrogen peroxide
HRR	homologous recombination repair
IR	ionizing radiation
IRIF	Ionizing Radiation Induced Foci
KAP1	Kruppel-associaated box (KRAB) associated protein 1
KO	knockout
KU-55933	ATM inhibitor
LET	linear energy
µl	microliter
MDC1	mediator of DNA damage checkpoint protein 1
Mdm2	the murine double minute 2
MEF	mouse embryonic fibroblast
Min	minute
Mre11	meiotic recombination 11 homology
MN	micronucleus
MRN	Mre11/Rad50/Nbs1
MSH	the mismatch DNA repair proteins
Nbs1	Nijmegen Breakage Syndrome protein
NHEJ	nonhomologous end joining
NSCLC	non-small cell lung cancer
O_2	oxygen
OH	hydroxyl group
$OH^{\bullet}$	hydroxyl free radical
8-OxoG	8-oxoguanine
PARP1	poly (ADP-ribose) polymerase 1

PBS	phosphate buffered saline
PG	phosphoglycolate
PI	propidium iodide
P13K	phosphatidylinositol-3-kinase related
PNKP	polynucleotide kinase/phosphatase
PO_4CH_2COOH	phosphoglycolate
pTyr	phosphotyrosyl
RAD50	family of RADiaton sensitive genes (50 homology)
RB	retinoblastoma
RNA	ribonucleic acid
ROS	reactive oxygen species
RPA	single-stranded DNA binding protein
SCAN1	spinocerebellar ataxia with axonal neuropathy
SCID	severe combined immune-deficiency
Sec	seconds
SDS	sodium dodecyl sulfate
SD	standard deviation
SEM	standard error mean
SSBs	single-strand DNA breaks
ssDNA	single-strand DNA
TDP1	Tyrosyl DNA-phosphodiesterase 1
Top1	topoisomerase I
UV	ultraviolet
V(D)J	variable, diversity, joining
WT	wild type
XLF	XRCC4-like factor
X4L4	xrcc4-DNA ligase IV complex

XRCC	X-ray cross complement protein

Abstract

ROLE OF TYROSYL-DNA PHOSPHODIESTERASE 1 (TDP 1) ON REPAIR OF 3′-PHOSPHOGLYCOLATE (3′- PG) TERMINATED DNA DOUBLE-STRAND BREAKS (DSBS) AND IN RESPONSE TO OXIDATIVE STRESS

By Tong Zhou, B. of Medicine

A thesis submitted in partial fulfillment of the requirements for the degree of Master of Science at Virginia Commonwealth University

Virginia Commonwealth University, 2012

Advisor: Lawrence F. Povirk, Professor, Department of Pharmacology and Toxicology

DNA DSBs are most toxic to cells because they can lead to genomic rearrangements and even cell death. Most DSBs induced by ionizing radiation or radiomimetic drugs such as calicheamicin and bleomycin, bear 3′-phosphate or 3′- PG moieties that must be removed to allow subsequent gap filling and ligation. DSBs can be repaired by two main pathways: the homologous recombination (HR) pathway and the non-homologous end-joining (NHEJ) pathway, NHEJ is the primary repair pathway in mammalian cells. While HR repairs single strand breaks (SSBs) or DSBs accurately by using an undamaged copy of the sequence mostly at late S phase and G2 phase, the NHEJ pathway repairs DSBs without the requirement for sequence homology in a processing that may be error-free or error- prone and is most active at G1 phase. TDP1 is a DNA repair enzyme in both pathways, It associates with DNA SSB repair proteins XRCC1 and DNA ligase III and plays a role in processing of topoisomerase I- mediated

SSBs. Our early results suggested that TDP1 also can remove protruding 3′- PG and other 3′ blocks from DSBs ends in vitro. A homozygous H493R mutation in the active site of TDP1 causes spinocerebellar ataxia with axonal neuropathy (SCAN1), a rare autosomal recessive genetic disease with neurological symptoms including peripheral neuropathy. DNA damage and misrepair can be determined by measuring the incidence of chromosomal aberrations such as rings, breaks, dicentrics, acentric fragments, and translocations in metaphase cells, and micronuclei in interphase cells. To assess the possible role of TDP1 in DSB repair in intact cells, the radiosensitivity of SCAN1 cells was determined by using a dose-fractionation method of irradiation. The data indicated that, when exposed to fractionated radiation doses, the SCAN1 cells were more sensitive than normal cells. Moreover, following treatment of cells with calicheamicin, SCAN1 cells showed a significantly higher incidence of dicentric chromosomes, acentric fragments, and micronuclei compared to normal cells, indicating that calicheamicin-induced DSBs were repaired less accurately and less efficiently, or more slowly in SCAN1 cells than in normal cells. All these results are consistent with a role for TDP1 in repair of 3′-PG DSBs in vivo.

Oxidative stress is thought to induce replicative senescence and DNA damage in mouse embryo fibroblasts (MEFs). To determine the possible roles of oxidative stress on Tdp1-deficient MEFs, Tdp1-knockout MEFs and normal MEFs were cultured in 20% oxygen (atmospheric) and 3% (physiological) oxygen. The data from growth assays indicated that normal MEFs showed replicative senescence in 20% oxygen but not in 3% oxygen. Tdp1-knockout MEFs showed very poor growth compared to Tdp1 normal MEFs in both oxygen conditions, clearly suggesting an influence of repair of Tdp1 on oxidative stress induced DNA-DSBs in MEFs.

Taken together, our results indicated that TDP1 is capable of removing protruding 3′-PG from DSB ends in intact cells. Moreover, DSBs induced by oxidative stress were repaired more slowly or inefficiently in MEFs when Tdp1 is absent, resulting in cell cycle arrest and poor cell growth.

I. INTRODUCTION

Cancer remains a leading cause of death globally. Along with surgery and chemotherapy, radiation therapy is one of the most important methods of cancer treatment. It contributes towards 40% of curative treatment for cancer (Baskar et al., 2012), and at least 50 percent of all cancer patients will receive radiotherapy at some stage during the course of their illness (Tobias JS et al., 1992). Although radiation therapy is directed at the tumor, it is inevitable that the normal tissues surrounding the tumor will also be affected by radiation damage (Burnet NG et al., 1996), and radiation is also a proven carcinogen. The target of radiation therapy is DNA.

1.1 DNA Structure

The structure of DNA forms the basis for discoveries in DNA damage and repair. In 1953, following a long term study and debate, the correct structure of DNA was resolved by Watson and Crick, their results were published in Nature on April 25, 1953 (Watson, Crick, 1953), and they were awarded a Nobel Prize in 1962 due to this work.

This classic description for the structure of DNA is that DNA has two helical chains coiled around each other on the same axis. The two chains are antiparallel and follow a right-handed helical pattern. The bases are on the inside, the phosphates are on the outside, and the deoxyribose sugar is roughly perpendicular to the attached base. As the phosphates are on the outside they have easy access to cations. There is a residue on each chain every 3.4 Å of axis length, and the structure repeats itself after 10 residues or 34 Å. The bases Adenine (Purine) bind with Thymidine (Pyrimidine) and bases Guanine (Purine) bind with Cytosine (Pyrimidine).

1.2 DNA Lesions

Although the structure of DNA is relatively stable as a carrier of hereditary information, DNA damage due to environmental factors or normal metabolic processes inside the cell occurs at a rate of 1,000 to 1,000,000 molecular lesions per cell per day (Lodish et al., 2004). Unrepaired lesions in critical genes (such as tumor suppressor genes) can impede a cell's ability to carry out its function and increase the likelihood of tumor formation. The majority of DNA damage affects the primary structure of the double helix. DNA lesions can be classified as endogenous and environmental.

Endogenous DNA damage may come from intracellular production of reactive oxygen species (ROS); from normal metabolic byproducts; especially from the process of oxidative deamination, also from V(D)J recombination as well as some replication errors. There are five main types of DNA lesions due to endogenous cellular processes: oxidation of bases (e.g. 8-oxoG), alkylation of bases (e.g. methylation), hydrolysis of bases (e g. deamination, depurination), bulky adduct formation and mismatch of bases (due to errors in DNA replication) (De Bont, van Larebeke, 2004).

Exogenous DNA damage may result from: exposure of ultraviolet light B (UV-B light causes crosslinking creating pyrimidine dimers, called direct DNA damage; UV-A light creates mostly free radicals), thermal disruption (causes increased rate of depurination and single strand breaks), industrial chemicals (e.g. hydrogen peroxide, polycyclic aromatic hydrocarbons), or exposure of ionizing radiation (causes bases oxidation, single-strand breaks and double-strand breaks) (Acharya et al., 1975). Base damage and SSBs can subsequently lead to DSBs when encountered by DNA replication or transcriptional machinery (Branzei & Foiani, 2007; Michel et al., 2004).

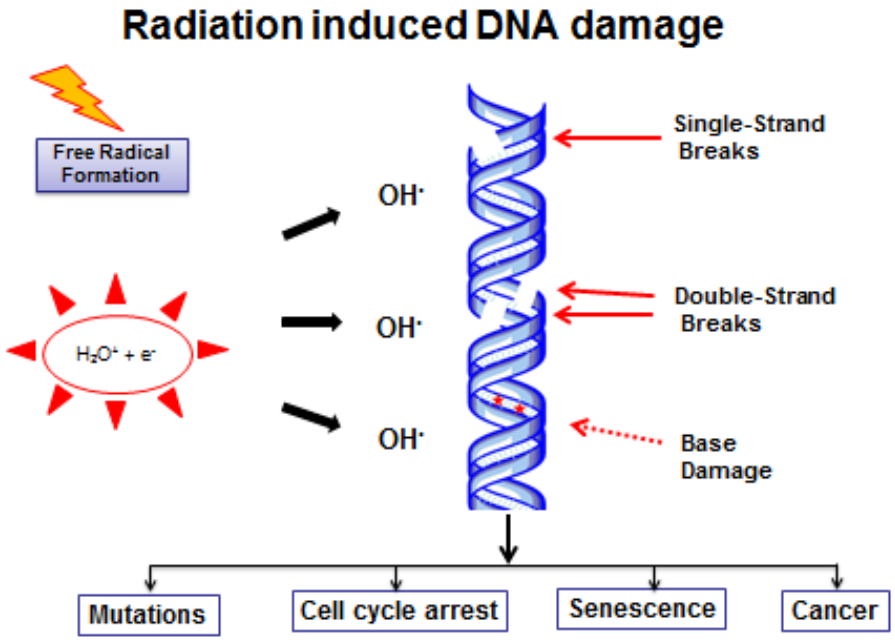

Figure1-1. Radiation-induced DNA damage. Radiation interacts with water, which constitutes 80% of the cell volume, to form hydroxyl radicals (OH·) that then account for the majority of the damage caused by γ-rays. The hydroxyl radical diffuses in aqueous solution and damages DNA and other cell components and induces a series of cell responses such as gene mutations, cell cycle arrest, and replicative senescence, and leads to the generation of cancer. Types of DNA damage induced by the hydroxyl radicals include single-strand breaks (SSBs), double strand breaks (DSBs), as well as base damage. There are several factors that affect which type of DNA damage would be generated, such as the proximity of the free radical generation to DNA, diffusion distance and the energy of the radical.

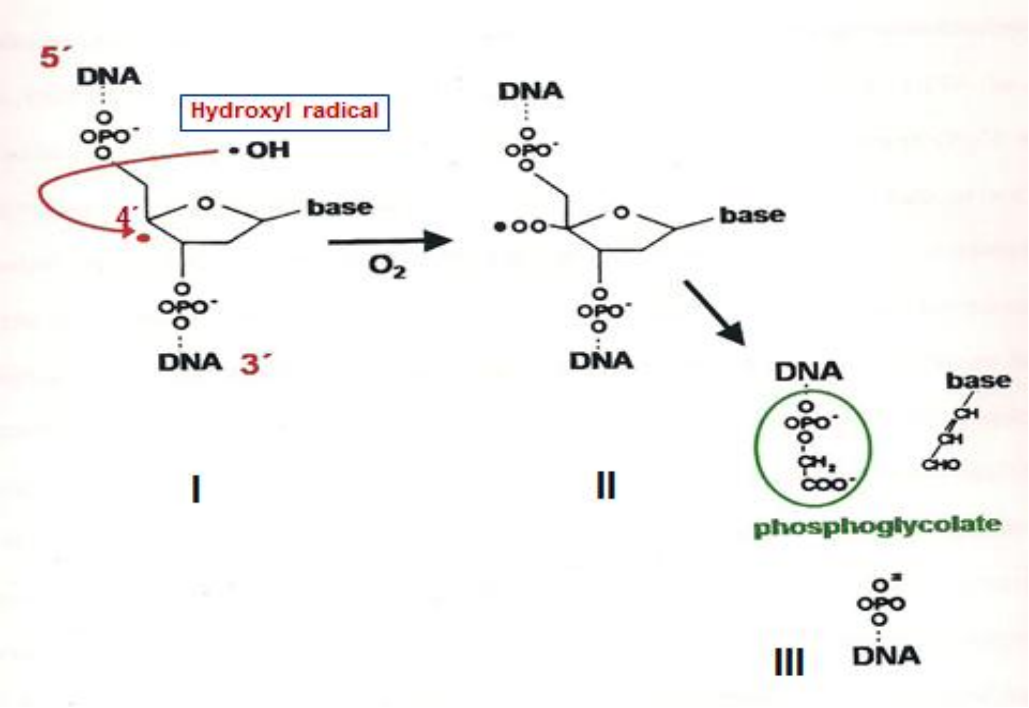

Figure 1-2.Formation of 3′**-Phosphoglycolate DNA end by ionizing radiation.** Radiation causes formation of free radicals. The free radical acts at the 4′-carbon of deoxyribose ring, changing the 4′-carbon into a radical species (I). The 4′ carbon radical then reacts with oxygen to become a peroxyl radical. Then the deoxyribose sugar spontaneously fragments (Giloni et al, 1981), creating a DNA break, releasing a base, leaving a phosphoglycolate bond to the 3′ carbon of the previous base in the DNA strand, and a phosphate bound to the 5′ carbon of the next base in the DNA strand.

1.3 Formation of 3′-Phosphoglycolate DNA End Modifications

Radical species from hydroxyl radical or superoxide radical attack the DNA chain on the 4′ carbon of deoxyribose, changing the 4′ carbon into a radical species. The radical 4′ carbon then reacts with oxygen to become an peroxyl species. Then the deoxyribose sugar spontaneously fragments (Giloni et al., 1981), creating a DNA break, releasing a base-propenal, a phosphoglycolate (PO_4CH_2COOH) bond to the 3′ carbon of the previous base in the DNA strand, and a phosphate bound to the 5′ carbon of the next base in the DNA strand. The radical species that may induce the attack mainly include hydroxyl radical HO• generated from the decomposition of H2O2 (Cadenas et al., 1989), or a superoxide radical O2.

1.4 Mechanism of Ionizing radiation-induced DNA double-strand break

Radiation used for cancer treatment is called ionizing radiation because it forms ions when passing through a tissue and cell. Most effects of ionizing radiation result from its damage to DNA (Hutchinson et al., 1966). Ions are atoms that have acquired an electric charge through the gain or loss of an electron (Dunne-Daly CF et al., 1999). Higher energy level of radiation (Linear Energy Transfer) such as α-particles, interact directly with critical biomolecules in cells like DNA to cause a change in the molecular structure. However, radiation may interact indirectly with water molecules in the cells, resulting in the production of highly reactive and unstable free radicals or reactive oxygen species, which immediately react with any biomolecules in the surrounding area, producing cellular damage (Fang YZ et al., 2002). The initial radical production following energy deposition is non-homogenous, and high local concentrations occur in events called clusters or spurs (6-100 eV for 1MeV electron) and blobs (100-500 eV for 1

MeV electron) (Mozumder, 1985). It is known that the interstrand distance (10 Å) can be spanned by regions of high radical density, making multiple radical attacks on opposite strands possible. These radical attacks in close proximity on both strands can lead to local multiply damaged sites (Complex DNA damage) (Ward, 1990), including DNA SSBs and DSBs, as well as some base damage like 8-oxoguanine (Demple, Harrison et al., 1994). SSBs and DSBs are produced in different proportions. While there are 1000 SSBs estimated for a Gy of radiation, about 40 DSBs occur per cell per Gy (Ward, 1990). DSBs are believed to be the most severe lesions that cause gene instability and cell death.

1.5 Cell Responses to DNA Damage.

It is extremely important to understand the various DNA damage responses that have evolved in cells to repair this damage, because even a single unrepaired DNA DSB can lead to cell death. A common hypothesis is that, following DNA DSBs, the first step in the cell response is to recognize the presence of damage, even though the mechanism directing the recognition of DNA DSBs remains unknown. ATM (Ataxia Telangiectasia Mutated), a main damage sensor, is activated by the presence of damage as well as changes in chromatin structure. Activated ATM phosphorylates H2AX yielding γ-H2AX) surrounding a DSB (Rogakou et al., 1998; Burma et al., 2001). MRN (Mre11/Rad50/Nbs1) complex is one of the first proteins that recruits and binds to broken DNA ends. Many other DNA damage response proteins are then recruited to the sites of DNA DSBs to form IRIF (Ionizing Radiation Induced Foci). Early IRIF are shown to consist of γ-H2AX, 53BP1 (a protein to function as a transcriptional coactivator with P53), MRN complex and MDC1 (mediator of DNA damage checkpoint protein 1, required to activate the intra-S phase and G/M phase cell cycle checkpoints in response to DNA damage), that reach peak levels at the IRIF within 30 min (Rogakou et al., 1998; Schultz et al., 2000) (Stewart et al.,

2003). Rad51, Rad52, BRCA1 and BRCA2 are involved in foci formed at later times following radiation exposure. ATM, BRCA1, MSH2, MSH6 (the mismatch DNA repair proteins), and MLH1, BLM and MRN complex are thought to form part of BASC (BRCA1-associated genome surveillance complex), which has also been considered as a damage sensing complex (Wang et al., 2000). Some studies suggested the roles of DNA-PK in cell cycle checkpoint controls (Woo et al., 1998), and in apoptosis in response to DSBs (Wang et al., 2002), both of which are less clear than those for ATM and ATR.

Once DNA damage is recognized, a choice for repair pathway needs to be made. There are two major mechanisms to repair DSBs in mammalian cells: HR and NHEJ (Valerie & Povirk, 2003; Lieber, 2008). Several factors that influenced the choice of pathway will be discussed in the following section.

1.6 Homologous Recombination (HR) Repair.

HR repair for DSBs requires homologous sequences, such as sister chromatids, as a template to replace lost nucleotides at the break site. Therefore, HR repair is considered a high fidelity or error-free pathway for repair of DNA DSBs, especially for those DSBs caused by replication forks collapse (Sung & Klein, 2006). This pathway is only active in late S and G2 phases of the cell cycle (Helleday et al., 2007; Takata et al., 1998). A large group of proteins are involved in HRR pathway and play different roles. These proteins include RAD51, RAD52, RAD54, RAD55, RAD57, BRCA1, BRCA2, XRCC2, XRCC3 and MRN complex. Following 5′-3′ resection, RPA (single stranded DNA binding protein), RAD51, RAD52 and RAD54 bind to resulting ssDNA overhangs (Li & Heyer, 2008). RAD51 and RPA on ssDNA tails help in initiating strand exchange. MRN complex, along with other nucleases (possibly CtIP) resect the

DNA to generate ssDNA ends for DNA pairing and strand exchange as well as holliday junctions form. Now either the Holliday junctions disengage and DNA strands pair or a crossing-over event may result from nucleolytic Holliday junction resolution. CtIP is involved in the required resection because it possesses a 5′-3′ exonuclease activity that MRN complex does not have. CtIP along with MRN has been shown to be required for the 5′ DNA end resection following which the ssDNA is bound by RPA and subsequent steps of HRR can occur.

1.7 Non-homologous End Joining (NHEJ) Repair

NHEJ is the predominant mechanism for DSBs repair in mammalian cells, mainly in G1/G0 phase of the cell cycle (Rothkamm et al., 2003). NHEJ is more effective in repair of DSBs induced by V(D)J recombination (Jankovic et al., 2007), and most particularly, it does not require homologous sequence information for repair (Roth, Porter & Wilson et al., 1985). Radiation and the resulting ROS interact with DNA to produce multiply damaged sites/complex DNA damage with different lengths of overhangs, termini blocked with 4′- oxidation products and several types of base damage most commonly 8-oxoguanine and thymidine glycols. Core NHEJ proteins include KU, DNA-PKcs, DNA ligase IV, its cofactor XRCC4 (Chu, 1997; Calsou et al., 1999; Karran et al., 2000; Chen S et al., 2001), DNA polymerase μ and λ (Mahajan et al., 2002) and XLF (Lieber, 2010).

1.7.1 Mechanism of NHEJ pathway.

Once DSBs occur, Ku heterodimers first bind to DSBs (Mimori, Hardin, 1986). Ku then binds to DNA-PK forming stable Ku: DNA-PK complex serving as a node where nucleases, polymerases and ligases can bind (Lieber, 2008). The change in conformation of Ku-DNA-PK complex in DNA ends may also facilitate interaction of Ku with DNA polymerases μ and λ along with

XRCC4: DNA ligase IV complex (Nick McElhinny et al., 2000; Chen et al., 2000). Upon synapsis of two DNA ends, DNA-PKcs autophosphorylates leading to its dissociation from the DNA ends so that other DSB repair proteins get access to the ends of DSBs (Weterings, 2007). TDP1 processes DSB ends with a variety of 3′- blocked overhangs. Artemis acts with its 3′ endonucleolytic activity to process 3′-PG terminated DNA DSB ends in presence of DNA-PK, to promote repair proficiency in mammalian cells (Mohapatra et al., 2011). Then the gap would be filled by polymerases μ and λ, and the ends are ligated by the XRCC4-DNA ligase IV complex (X4L4), which is stimulated by interaction between XLF and XRCC4. For a small part of more difficult DSBs, such as DSBs with long or severe damaged termini; DSBs in heterochromatin; or DSB whose ends have become physically separated, some other proteins in the "repair foci", including ATM kinase, 53BP1, MRN complex, and Artemis, might be required in a more complex subpathway of NHEJ (reviewed in Valerie & Povirk, 2003).

1.7.2 Structural and biochemical properties of core NHEJ proteins

Ku

Ku is a heterodimer consisting of a 70 kDa (Ku70) and a 86 kDa (Ku80) subunit (Walker, Corpina & Goldberg 2001; Valerie, Povirk, 2003) which was first identified as an autoantigenic protein from a scleroderma patient with initials K.U. The ring shape of Ku is consistent with the property of Ku to bind DNA ends and its ability to slide internally allowing other DNA repair proteins access to DNA ends (Mimori, Hardin, 1986). X-ray crystallography studies have shown that Ku occupies approximately 16 bp of double helical DNA at DNA ends (Walker, Corpina & Goldberg, 2001). The two subunits interact with each other through their carboxyl-terminal domains. A minimum of 28 amino acids in the center of Ku80 are critical for Ku heterodimer complex formation (Wu, Lieber, 1996). It also has more affinity for double strand DNA than single strand DNA (Tuteja et al., 1994). Neither subunit alone can bind to DNA efficiently suggesting that Ku70 and Ku80 functions are

interdependent. Ku has also been shown to form a bridge between DNA ends that may help in aligning the two ends together for carrying out further steps of repair (Ramsden, Gellert et al., 1998). It recruits DNA-PK to DNA ends, which then occupies extreme ends of DNA (Yoo, Dynan, 1999). DNA-PK holoenzyme complex occupies approximately 30 bp from the DNA end as suggested by DNase footprinting. In addition to DNA alignment and facilitation of DNA-PK recruitment, Ku was identified as an effective 5′-dRP/AP lyase and was found essential for the removal of AP sites near DSBs (Roberts et al., 2010).

DNA-PK

DNA-PK belongs to the family of phosphatidylinositol-3 kinases (PI3Ks) and is a large protein with a molecular weight of 469 kDa (Hartley et al., 1995). Its kinase activity is specifically activated by binding to duplex DNA ends (Smith, Jackson, 1999). The DNA-PK:Ku holoenzyme binds to blunt DNA ends much tightly than does DNA-PK alone (West, Yaneva & Lieber, 1998), suggesting that Ku facilitates DNA-PK binding to DNA ends. However, DNA-PK catalytic subunit can bind to DNA in the absence of Ku and the binding is competitively inhibited by ssDNA or supercoiled DNA (Hammarsten, Chu, 1998; Hammarsten, DeFazio & Chu, 2000). This suggests that DNA-PK can be activated by its direct interaction with dsDNA and Ku is needed to stabilize DNA-PK binding. Once bound, DNA-PK acquires S/T kinase activity (Hartley et al., 1995), and one of its initial targets is DNA-PK itself, with more than 15 autophosphorylation sites already identified (Meek, Dang & Lees-Miller, 2008). Two major autophosphorylation clusters have been extensively studied and span residues 2609-2647 and 2023-2056. This autophosphorylation of the two end-bound DNA-PK may lead to its dissociation from DNA ends to allow further processing (Valerie, Povirk, 2003; Karran, 2000). Several studies indicate that overhangs are more robust activators of the DNA-PK kinase activity than DNA ends with blunt DNA termini (Hammarsten, DeFazio & Chu, 2000; Smider et al.,

1998; Jovanovic, Dynan, 2006). DNA-PK preferentially phosphorylates serine and threonine sites followed by a glutamine (S-T/Q sites). Most of the known NHEJ factors XRCC4, KU 70/80, Artemis, and XLF are excellent targets of DNA-PK *in vitro* and *in vivo*. DNA-PK-mediated autophosphorylation is critical for Artemis endonucleolytic activity. Activated DNA-PK has also been shown to stimulate the ligase activity of XRCC4: DNA ligase IV complex (Meek, Dang & Lees-Miller, 2008).

XRCC4/DNA Ligase IV/XLF

The XRCC4 gene was originally identified by complementation of radiosensitivity and DSB repair deficiency of the CHO derivative XR-1 (Li et al., 1995). Crystal structure of XRCC4 has revealed that four XRCC4 monomers form a dumb-bell shaped homotetramer with two globular heads and four tails that interact with each other. Both XLF and DNA ligase IV are present in a complex with XRCC4. (Lee et al., 2000). DNA ligase IV is present in a tight complex with XRCC4 in cells (Lee et al., 2000), and ligase IV is not detectable in cells lacking XRCC4 (Bryans et al., 1999). Ligase IV binds to XRCC4 at a site near the middle of the α-helical tail (Sibanda et al., 2001). It consists of N-terminal core catalytic domain and a carboxyl terminal domain with two tandem copies of BRCT (Callebaut et al., 2006) and it interacts with XRCC4 through the BRCT domains (Critchlow et al., 1997). The crystal structure of XLF (Cernunnos) suggests a similarity to the structure of XRCC4 (Andres et al., 2007). Interaction between XRCC4 and XLF was identified through a yeast two hybrid system that led to the discovery of XLF (Ahnesorg et al., Smith & Jackson et al., 2006). Deficiency of XLF in humans leads to radiosensitivity with associated microcephaly (Buck et al., 2006) and a lack of V(D) J recombination. XLF-deficient cells also fail to rejoin a substantial fraction of radiation-induced DSBs. *In vitro* reactions with purified proteins have shown XLF to stimulate ligation by X4L4.

Our lab has shown that alignment based gap filling is completely dependent on XLF in whole cell extracts suggesting that Cernunnos not only stimulates ligation by ligase IV, but may also be important for DNA alignment (Akopiants et al., 2009). DNA-PK inhibitor (KU57788) inhibits end joining mediated by XLF suggesting that presence of XLF and catalytically active DNA-PK is required for end-joining while ATM inhibitor KU55933 has no effect on the XLF-mediated end joining reaction (Akopiants et al., 2009). Contacts between KU and DNA ligase IV, and between DNA-PKcs and XRCC4 mediate binding of XRCC4/ligase IV to DNA-PK at the DNA end termini (Valerie, Povirk, 2003; Hsu, Yannone & Chen, 2001). DNA-PKcs phosphorylates XRCC4 on serine / threonine residues in the carboxyl terminal region of the protein (Leber et al., 1998), however, the relevance of this phosphorylation to NHEJ is still not clear. Analysis of the effect of DNA-PKcs on ligation by XRCC4/ligase IV complex shows that both proteins bind to the same DNA molecule and that such binding promotes intermolecular ligation as opposed to intramolecular ligation seen with XRCC4/ligase IV complex alone (Chen et al., 2000). These studies suggest that XLF/XRCC4/ligase IV may serve as an alignment factor to bind DNA ends together allowing for ligation to proceed following repair by NHEJ.

Artemis, WRN, and MRE11 are all nucleases with putative roles in end-joining. Artemis has intrinsic 5′ -3′ exonuclease activity, and upon phosphorylation by DNA-PK obtains an endonuclease activity capable of opening hairpin loops, removing 5′ overhangs and shortening 3′ overhangs (Ma et al., 2002). WRN and MRE11 are 3′ -5′ exonucleases with a preference for recessed 3′ ends (Kamath-Loeb et al., 1998; Cooper et al., 2000; Li and Comai et al., 2000; Paull and Gellert et al., 2000; Trujillo et al., 1998) and WRN is stimulated by Ku (Cooper et al., 2000; Li and Comai et al., 2002).

1.8 Choice of DSB repair pathway

Cells have developed their ability to decide which DSB pathway to chose so that the damage can be optimally repaired and diminished. Several factors that affect the choice of DSB repair pathway mainly including the cell cycle phases, DNA end resection extent, and the severity and type of the DNA damage (Aylon et al., 2004; Huertas et al., 2008). In general, HRR may play a more role in late S and G2 phases as sister chromatids are more likely to be acquired during these two phases. During DNA replication, HRR is believed to be more important than NHEJ (Haber et al., 1999; 2000). NHEJ is available through the cell cycle but more active in G1/G0 phases. In mammalian cells, NHEJ has been reported to be a main repair pathway (Guirouilh-Barbet et al., 2004).

1.9 TDP1 (Tyrosyl-DNA phosphodiesterase)

RNA transcription, DNA replication, as well as other normal cellular processes produce DNA supercoiling (Liu and Wang et al., 1987). DNA topoisomerase I, a DNA untwisting enzyme, relieves DNA supercoiling by creating transient single-strand breaks (SSB) in which Tyr723 of topoisomerase is covalently linked to the 3′ end of DNA (Pourquier et al., 2001). TDP1 is a DNA repair enzyme that cleaves these tyrosyl-phosphate linkages in the rare instances where topoisomerase fails to religate the break and dissociate (Interthal et al., 2001). These rare instances include slowing the rejoining step or enhancing the initial formation of the cleavage complex, as well as accumulation of DNA lesions, such as oxidative damage and thymine dimers (Pourquier et al., 1999), and mismatched base pairs (Pommier, 1998). The phosphate group left by TDP1 would be removed by PNKP (polynucleotide kinase/phosphatase) (Yang et al., 1996). In vitro, TDP1 also processes protruding 3′-PG termini on DSB ends induced by oxidative stress (Inamdar et al., 2002) and other 3′-modifications (Interthal et al., 2005). TDP1 interacts with SSB repair proteins, but it is more active on DSB ends (Raymond et al., 2005). Even though

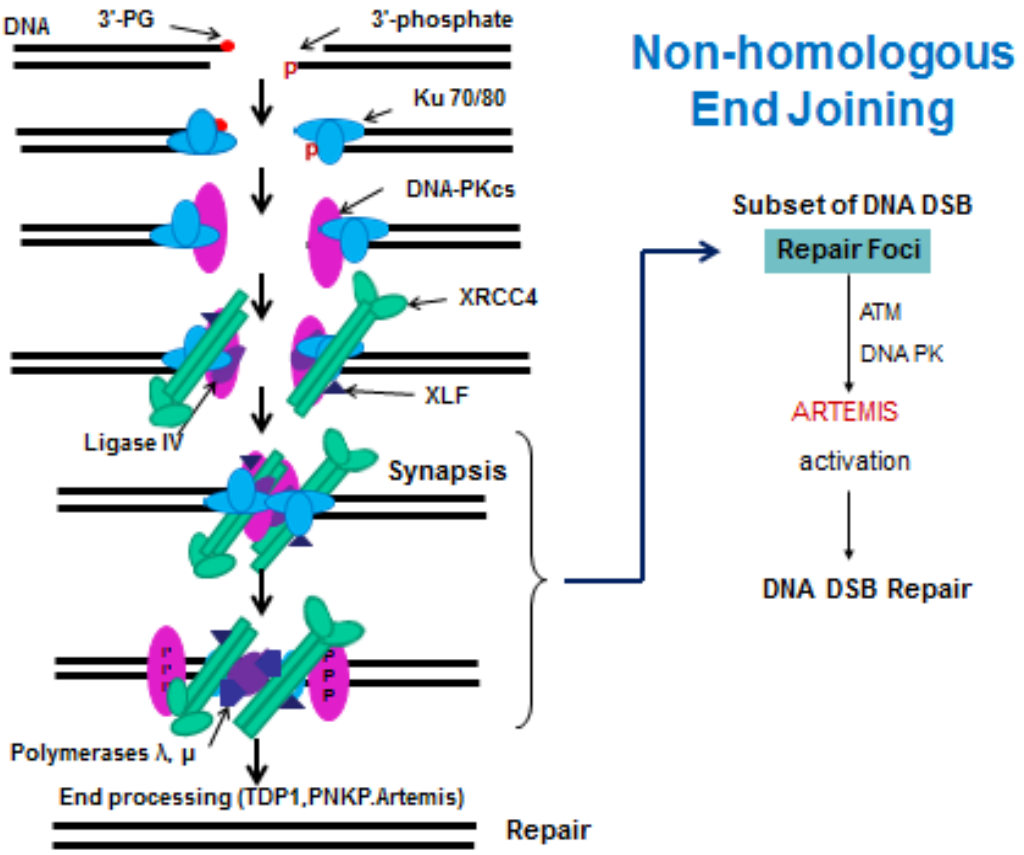

Figure 1-3. Nonhomologous end-joining repair. The Ku 70/80 heterodimer forms a ring structure (blue) that binds to DNA DSB ends. Bound Ku70/Ku 80 helps in the recruitment of DNA-PK (pink). This is followed by the recruitment of XLF : XRCC4 : DNA ligase IV to the DNA ends which in turn leads to the synapsis of the two ends. DNA-PK autophosphorylation causes a conformational change causing it to move away from the DNA-termini, allowing Artemis and other endonucleases to process the ends before gap filling by polymerases λ, μ, and ligation mediated by DNA ligase IV. (Adapted from Dr. Povirk's radiobiology lectures).

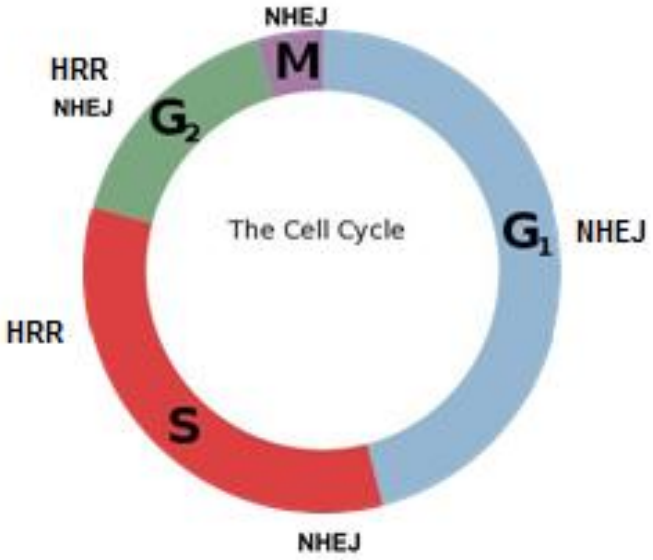

Figure 1-4. Cell cycle Dependence of DNA Repair. NHEJ is active throughout the cell cycle while HRR requires homologous DNA template in the form of sister chromatids (present in S and G2 phases) or repeated DNA sequences.

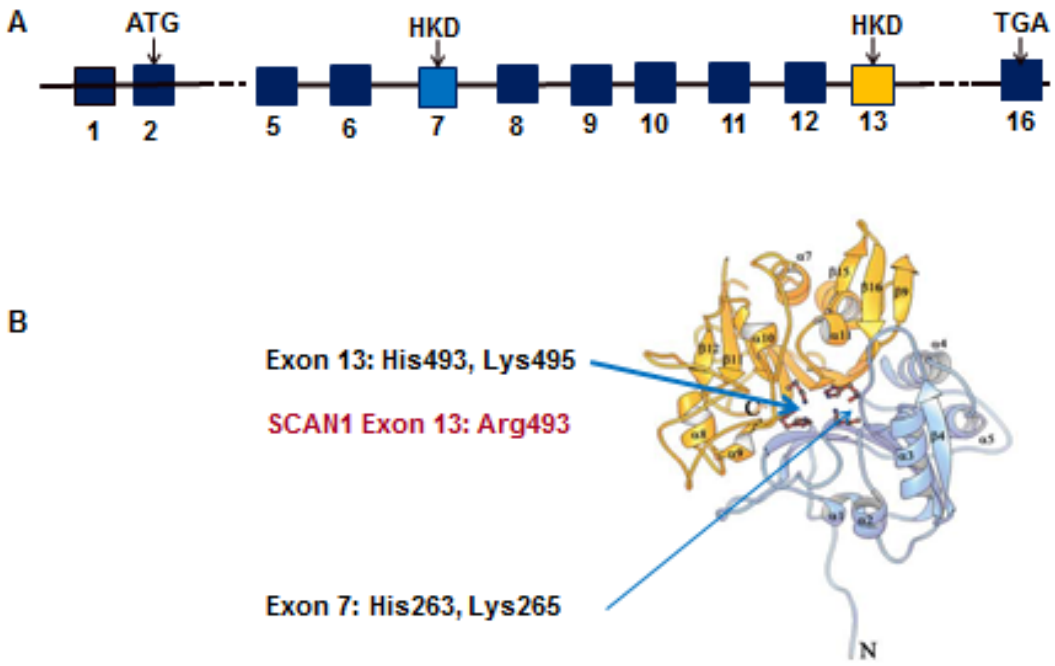

Figure 1-5. Diagram of the TDP1 gene and crystal structure of the Tdp1 protein gene product. A**.** The TDP1 gene is located at 14q32.11. B. The crystal structure as determined by Davies is colored by domain, with the N-terminal domain (residues 162-350) colored light blue and the C-terminal domain (residues 351-608) colored yellow. The active site is located along a pseudo-2-fold axis of symmetry between the two domains. The active site resides His263, Lys265, His493, and Lys495 are shown as ball-and-stick structures and are colored red (Davies et al, 2002).

APE1 (apurinic/apyrimidinic endonuclease) can remove 3′-PG moieties from blunt or 2-base-recessed DSB ends, only TDP1 is able to process protruding 3′-PG termini on DSB ends *in vitro* (Inamdar et al., 2002). Our studies also suggested that this in vitro removal of protruding 3′-PG was an early event in NHEJ that occurred prior to Ku loading or formation of the DNA-PK complex on DNA ends (Chen et al., 2001; Inamdar et al., 2002). Removal of the glycolate left a phosphate group, which was then removed by PNKP (Yang et al., 1996). A homozygous mutation at the active site of TDP1 has been identified as the cause of hereditary spinocerebellar ataxia with axonal neuropathy (SCAN1). The extract-based experiment suggested a deficiency in processing protruding 3′-PG termini on DSBs (Zhou et al., 2005). However, an *in vivo* experiment showed that SCAN1 lymphoblasts were no more sensitive to bleomycin (which specifically induces blunt 3′-PG termini) than wild-type cells (Interthal et al., 2005).

APE1 (apurinic/apyrimidinic endonuclease) is another enzyme that is responsible for certain types of 3′-PG removal. It is a major enzyme in the BER pathway responsible for removing apurinic/apyrimidinic (AP) sites, it also can remove 3′-PG from SSBs both with gaps and with internal nicks with no missing bases, and from DSBs with either blunt or 2-base recessed 3′-PG (Suh et al., 1997). However, APE1 did not show any detectable activity for processing PG on 1 or 2-base 3′-PG overhangs (Suh et al., 1997). Like all other members of the phospholipase D (PLD) superfamily, Tdp1 has two HKD motifs (HKD sequence) that come together to form a single active site (Stuckey & Dixon, 1999). The crystal structure of human TDP1 shows that HKD motifs are composed of histidines 263 and 493 and lysines 265 and 495, and that these resides are required for normal catalytic activity (Davies et al, 2002, Interthal et al., 2001, Raymond et al., 2004). Tdp1 reacts with its substrate through two Sn2 reactions (Stuckey & Dixon, 1999) and follows a general acid/base catalytic mechanism. First, H263 acts as a

nucleophile, leading to the formation of a phosphoamide bond to the 3′ end of the DNA moiety. Second, H493 acts as a base, activating a water molecule that hydrolyzes the reaction intermediate, leaving DNA with a 3′ phosphate end (Intelthal et al., 2001). The mutant TDP1 in SCAN1 has an arginine substituted for the H493 residue, and even though this mutant TDP1 has some remaining activity, it is much less than wild-type purified TDP1 (Intethal et al., 2005). The reduced catalytic activity of SCAN1 Arg493 is due to its failure to activate a water molecule at the active site of TDP1 (Interthal et al., 2005). The resulting effect in SCAN1 is that attempted repair of covalently-bound TOP1 by mutant TDP1 just exchanges TOP1 with covalently-bound mutant TDP1, which has a relatively long half-life compared to wild-type TDP1 which has an unmeasurably short half-life (Interthal et al., 2005). The resistance of covalently-bound TOP1 and mutant TDP1 on DNA may contribute to the molecular pathology of SCAN1.

1.10 Spinocerebellar Ataxia with Axonal Neuropathy (SCAN1).

SCAN1 is inherited as an autosomal recessive disorder, with onset at adolescence. TDP1 in SCAN1 has a homozygous H493R mutation in its active site (Takashima et al., 2002). SCAN1 patients show distal muscle weakness, gait disturbances, deep tendon reflexes absence, and mild brain atrophy (Takashima et al., 2002). Nine SCAN1 patients have been identified from a single large Saudi Arabian family, and no increased predisposition for cancer has been found thus far. Moreover, whole cell extracts isolated from lymphoblast cell lines of SCAN1 patients show a deficiency in processing protruding 3′-PG termini on DSBs, suggesting that processing protruding 3′-PG termini is fully attributable to TDP1 at least in vitro (Zhou et al., 2005). It is generally presumed that SCAN1 pathology is due to the failure of mutant TDP1 to efficiently repair topoisomerase I- associated DNA damage (Takashima et al., 2002). This repair deficiency

could indirectly confer sensitivity to oxidative DNA damage, which tends to promote formation of topoisomerase I cleavage complexes (Pourquier et al., 1999). Upon replication these cleavable complexes can be converted to toxic topoisomerase-terminated DSBs (Hsiang et al., 1989). Furthermore, SCAN1 pathology is similar to two other neuronal diseases, Freidreich ataxia and ataxia with oculomotor apraxia (AOA1) (Caldecott et al., 2003), both of which have been linked to oxidative damage. Even though not proven, some lines of circumstantial evidence suggest possible relationships among TDP1 deficiency, oxidative damage, DSBs and SCAN1 pathology.

1.11 Chromosome Aberrations and Micronuclei

Chromosome aberrations. Chromosomes are composed of long molecules of DNA. When cells are exposed to radiation or carcinogens, DNA sometimes breaks, and the broken ends may fail to rejoin or may rejoin in different patterns from their original arrangement. The abnormalities that result are termed "chromosome aberrations" and may be visualized at mitosis when cells divide. Chromosome aberration reflects an atypical number of chromosomes (numerical disorders also called aneuploidy) or a structural abnormality in one or more chromosomes. The frequency of chromosome aberrations increases with radiation dose to the cells and serves as an indicator of radiation dose received. Chromosome breaks, exchanges (rings), dicentrics, and translocations are some examples of chromosome aberrations. Among different types of aberrations, dicentrics and acentrics (chromosome fragments) are relatively easy to detect, and their frequency is therefore useful as indicator for chromosome damage (Nakano et al., 2001, 2007; Kodama et al., 2001, 2005; Ohtaki et al., 2004).

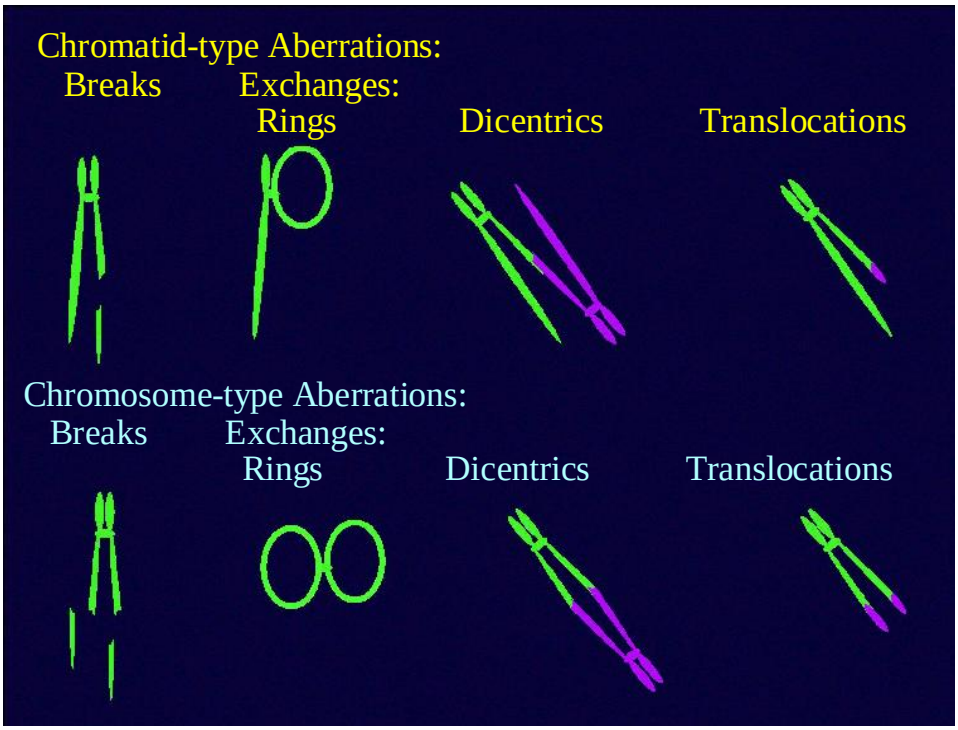

Figure 1-6. Chromosome aberrations (a model generated by Dr. Povirk). Ionizing radiation and radiomimetic agents cause damage of DNA. This damage can be repaired by NHEJ pathway which is error-prone. Acentric fragments indicate chromosome breaks, rings, dicentrics, and translocations indicate misrepairs which are easy to detect.

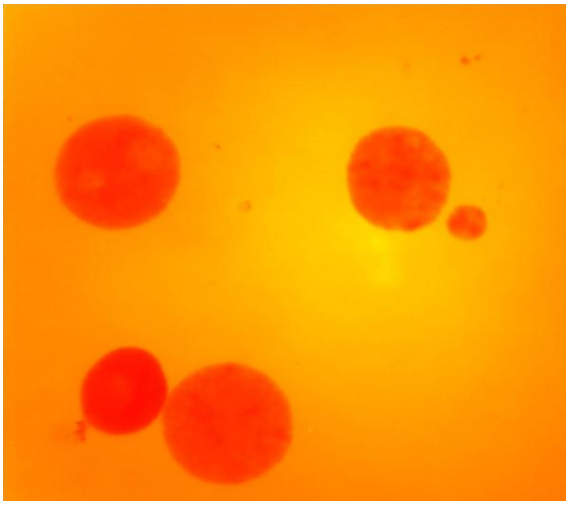

Figure 1-7. Micronucleus formation. A micronucleus (MN) is formed during the anaphase of mitosis or meiosis. Micronuclei are cytoplasmic bodies having a portion of acentric chromosome or whole chromosome which was not carried to the opposite poles during the anaphase. Their formation results in the daughter cell lacking a part or all of a chromosome. These chromosome fragments or whole chromosomes normally develop nuclear membranes and form micronuclei as a third nucleus. After cytokinesis, one daughter cell ends up with one nucleus and the other ends up with one large and one small nucleus, i.e., a micronucleus. There is a chance of more than one micronucleus forming when more genetic damage has happened. The micronucleus test is used as a tool for genotoxicity assessment of various DNA damage components and radiation. It is easier to conduct than the chromosomal aberration test in terms of procedures and evaluation.

Micronuclei. A micronucleus (MN) is formed during the anaphase of mitosis or meiosis. Micronuclei are cytoplasmic bodies having a portion of acentric chromosome or whole chromosome which was not carried to the opposite poles during the anaphase. Their formation results in the daughter cell lacking a part or all of a chromosome. These chromosome fragments or whole chromosomes normally develop nuclear membranes and form as micronuclei as a third nucleus. After cytokinesis, one daughter cell ends up with one nucleus and the other ends up with one large and one small nucleus, i.e., a micronucleus. There is a chance of more than one micronucleus forming when more genetic fragment broken off from a chromosome. The micronucleus test is used as a tool for genotoxicity assessment of various DNA damage components and radiation. It is easier to conduct than the chromosomal aberration test in terms of procedures and evaluation.

1.12 Types of DSBs caused by ionizing radiation, free radical species, and Calicheamicin.

Calicheamicin. Calicheamicins are a class of enediyne antibiotics, derived from the bacterium Micromonospora echinospora, calicheamicin γ1 is the most notable one, it was isolated from the chalky soil in mid-1980's (Lee et al., 1989). Activated Calicheamicin forms a diradical species that simultaneously attacks both strands of DNA with a 3-base 3′ stagger (Dedon et al., 1992). One end of each calicheamicin-induced DSB has a 5′ -phosphate, and 3-base 3′ overhang with a 3′ -phosphate. The opposite DSB end has a 5′ -aldehyde and a 2-base protruding 3′overhang with either a 3′-phosphate or a 3′-PG.

Ionizing radiation. DSBs induced by ionizing radiation generate many kinds of DSB ends. It has been estimated that 10-50% of DSBs (Hutchinson et al., 1985; Bradbury et al., 2003) have 3′-PG termini, presumably about half protruding and half recessed 3′-PG termini.

Diffusible free radical species from many sources. These free radical species-induced DSBs usually have 5′ -phosphate (occasionally 5′ -hydroxyl) termini, while the 3′ ends will be blocked by phosphates or by deoxyribose fragments, most commonly 3′ -phosphoglycolate (-PO_4CH_2COOH; PG) (Isildar et al., 1981; Henner et al., 1983; Ward et al.,1988).

1.13 TDP1 as a target in cancer therapy.

While DNA damage underlies carcinogenesis, it can also be utilized as a means of cancer treatment. The capacity of cancer cells to recognize, process and repair DNA damage is a key mechanism for therapeutic resistance to chemotherapy (Dexheimer et al., 2008). Due to its role in processing of irreversible Top1-DNA covalent complexes, TDP1 has been regarded as a potential therapeutic co- target of Top1, also in that it seemingly arrests the effects of Top1 inhibitor, such as camptothecin (CPT). Therefore, by reducing the repair of Top1-DNA lesions, Tdp1 inhibitors have the potential to enhance the anticancer activity of a Top1 inhibitor, especially in tumor cells where there may be genetic abnormalities that could confer deficiencies in alternative repair pathways. Studies performed in SCAN1 cells have further established proof of principle for the development of Tdp1 inhibitors in combination with CPT in anticancer drug therapy. Homozygous mutant SCAN1 cells have been shown to accumulate more total DNA strand breaks than normal lymphoblastoid cells after treatment with CPT (EI-Khamisy et al., 2005; Miao et al., 2006). SCAN1 cells have also demonstrated enhanced sensitivity to the killing effects of CPT (Interthal et al., 2005; Miao et al., 2006). Furthermore, complementary studies have shown that overexpression of wild-type Tdp1 protects cells against CPT-induced cell death (Barthelmes et al., 2004; Nivens et al., 2004), whereas the inactive mutant Tdp1 H263A does not (Barthelmes et al., 2004). Moreover, TDP1 expression has been shown to be elevated in non-

small cell lung cancer (NSCLC), a cancer commonly treated with CPT (Liu et al., 2007). Thus, inhibition of Tdp1 can be envisioned to potentiate the cytotoxic effects of the clinically used Top1 inhibitors.

A Tdp1 inhibitor aminoglycoside neomycin has been found to inhibit the activity of TDP1 (Liao et al., 2006). This drug was originally found based on its reported ability to inhibit phospholipase D (PLD) (Huang et al., 1999). Both Vanadate and tungstate were found to be able to inhibit Tdp1 due to their ability to mimic the transition state of Tdp1, however, they cannot be used as pharmacological inhibitors because of their broad activity against phosphoryl transfer reactions. For the discovery of novel Tdp1 inhibitors, the potential candidates should enhance the cytotoxicity of CPT and delay the removal of Top1 cleavage complexes in cell culture, in other words, the new drugs should selectively enhance the activity of Top1 inhibitors in tumors with preexisting DNA repair and cell cycle checkpoint deficiencies (Dexheimer et al., 2008).

1.14 Specific aims for this part.

TDP1 has been indicated in its role in processing 3′-PG and other 3′ termini on DSB ends induced by oxidative stress in vitro (in both whole cell extract and nuclear extract of TDP1-mutant SCAN1 and normal control cells). In order to assess the biological significance of 3′-PG processing by TDP1, radiosensitivity of TDP1-mutant SCAN1 cells was determined, chromosome aberrations also were examined following treatment of normal and TDP1-mutant SCAN1 cells with calicheamicin which specifically causes 3′-PG DSBs.

1.15 Oxidative Stress and Replicative Senescence

Oxidative stress is an imbalance between the production of reactive oxygen species (ROS) and the ability of the biological system to repair the resulting damage. One source of reactive oxygen

species under normal conditions in humans is the leakage from mitochondria during oxidative phosphorylation. Oxidative stress causes extensive DNA damage through production of ROS, which form peroxides and free radicals, disturb normal redox state of cells, activate cell signaling, trigger apoptosis, and even cause cell necrosis and death. Cellular replicative senescence is regarded as a result of oxidative stress (Parrinello, 2003). Replicative senescence affects the proliferation of many cell types (Parrinello et al., 2003). Replicative senescence in human cells is induced mainly due to telomere shortening when replicated in the absence of telomerase. DNA damage and activation of certain oncogenes also cause cellular senescence (Shelton et al., 1999). MEFs are able to spontaneously overcome replicative senescence to become immortal. MEFs senescence depends predominantly on the p19 ^{AFR}/p53 tumor suppressor pathway, whereas human fibroblasts need to lose both p53 and retinoblastoma (Rb) tumor suppressor functions for immortalization (Kamijo et al., 1997). MEFs senesce despite having long stable telomeres (Wright et al., 2000). It was reported that senescent MEFs showed an enlarged and flattened cell morphology and expressed senescence-associated beta-galactosidase (Chen et al., 2001). As mentioned above, p53 and Rb are two main activators of senescence. MEFs' senescence depends predominantly on the p19 ^{AFR} / p53 tumor suppressor pathway. Oxidative stress and DNA damage induce phosphorylation of ATM/ATR, two important DNA damage sensors. The phosphorylation of ATM/ATR further activates p19 ^{ARF} protein, and subsequent activation of chk1/chk2, and finally phosphorylation of p53. P19 ^{ARF} protein activates p53 by sequestering Mdm2, an E3 ubiquitin ligase in the nucleolus, preventing the Mdm2-mediated degradation of p53. P53 protein is stabilized and proceeds to activate its transcriptional targets (Kulju & Lehman, 1995). These targets act as majority of effectors involved in cell-cycle progression.

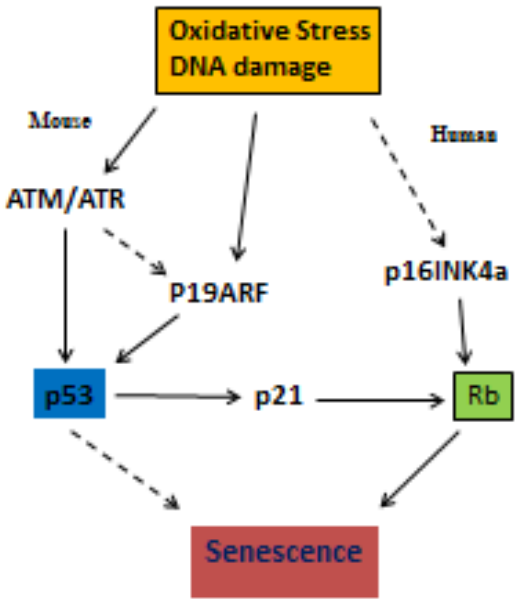

Porath et al., 2005

Figure1-8. Signals and pathways activating cellular senescence in MEFs. Telomere uncapping induces senescence mainly through the DNA damage pathway, activating the ATM/ATR pathway and Chk1/Chk2 to stabilize p53. In mouse this response is dependent on the activity of p19ARF, while in humans the role of ARF in this response is not known. In human cells p16 is activated in certain settings in response to telomere uncapping, through unknown pathways. Direct DNA damage activates the senescence program mainly through p53, in essentially the same manner as telomere uncapping. Oxidative stress induces DNA damage, and also accelerates telomere shortening, possibly leading to accelerated telomere uncapping. The downstream response is mediated through the DNA damage pathway and through $p19^{ARF}$. Activation of p16 by oxidative stress is seen in certain conditions mainly in human cells (adapted from Ben-Porath et al., 2005).

P53 activates senescence also by activating Rb through p21, an inhibitor of cyclin E/Cdk2 complexes. Rb activates senescence by turning off the transcription of E2f target genes (Narita et al., 2003). Both p53 and Rb are necessary for the initiation of senescence (Dannenberg et al., 2000; Sage et al., 2000). Activated p53 and Rb are required to maintain MEFs in senescent state, otherwise the MEFs will resume a proliferating state (Dirac and Bernards, 2003; Sage et al., 2003).

1.16 Specific aims

When we assessed the radiosensitivities of immortal Tdp1 mouse cells, we found that there were no differences between Tdp1 normal and Tdp1 deficient cells, we thought that may be this is caused by the possible occurrence of a mutagenic or adaptive event in MEFs in 20% oxygen. So we began to culture early passage of Tdp1 MEFs at normal culture conditions, including 20% oxygen. We found that Tdp1 deficient MEFs did not form colonies and grew very poorly in 20% oxygen. In order to assess the role of oxidative stress on Tdp1 deficient MEFs, Tdp1 normal and Tdp1 deficient MEFs were cultured in 20% and 3% oxygen and the lifespan, growth, and various DNA damage and damage response endpoints were examined.

II. MATERIALS AND METHODS

2.1 SCAN1 cells culture and radiosensitivity assay.

Cell lines from SCAN1 patients and from unaffected members of the same family were generated by transfection of peripheral lymphocytes with Epstein-Barr Virus (Takashima et al., 2002), and initially acquired from Dr. James Lupski (Baylor College of Medicine). These cells were maintained in suspension in upright T-75 cm^2 flasks at a density of 10^5-10^6/ml in RPMI 1640 medium (Gibco) including 10% fetal bovine serum and antibiotics.

For radiosensitivity assays of cells from SCAN1 patients and normal relative, the cells were grown to plateau phase (around 2 x 10^6/ml) in 24 – well plates and irradiated with 0.4 – 1.6 Gy ^{137}Cs γ-rays each day for 5 days. Then cells were diluted to 10^5 /ml and the concentration of viable cells as judged by trypan blue-exclusion of each sample was measured every other day for 19 days.

2.2 Dose – Fractionation

Dividing a single dose of radiation into multiple smaller doses is referred to as dose fractionation. In this radiosensitivity assay, dose fractionation method was used to allow the normal cells to repair damaged DNA during time intervals between doses, while the cells with absence of DNA repair function will cycle into a more sensitive phase between treatments, rendering them more susceptible to radiation damage.

2.3 Cytogenetics- preparation of metaphase spreads and centromeric hybridization

Epstein-Barr virus-transformed lymphoblastoid cells of SCAN1 patients and unaffected relatives were obtained from Dr. James Lupski (Baylor College of Medicine), and maintained in RPMI1640 medium with 10% FBS and antibiotics. Calicheamicin was obtained from Wyeth Pharmaceuticals as a gift, and was dissolved in ethanol and regularly stored at -80°C. It was diluted to 20 µM in Dimethyl Sulfoxide (DMSO) and then diluted in complete medium prior to use. 0-30 pM calicheamicins were used to treat cells for 24 hours and 1 µg/ml colchicine (due to its mitosis-inhibiting function) was added 2 h before harvest. Metaphase spreads were prepared by standard procedures: Cells were trypsinized as normal and washed with 1 x 10 ml PBS in 15 ml tubes. Then 0.075 M KCl was slowly added dropwise to 10 ml. As soon as there were about 3 ml of KCl in the tube addition became faster and the tube was gently inverted during the addition of KCl. Cells were incubated at 37 °C (in a water bath) for 6 minutes. Cells were centrifuged at 900 rpm for 5 minutes. Remove as much KCl as possible and gently resuspend the cells in the residual. Slowly add 3 ml of fixative (3:1 Methanol / Acetic acid; prepared fresh) dropwise and carefully mix the whole time (Adding fixative too quickly will result in clumping). Cells were centrifuged at 900 rpm for 5 minutes and fixative was removed. Cells were centrifuged at 900 rpm for 5 minutes again and the fixative was removed. Cells were dissolved in 200-500 µl fixative (cells are stable for extended times in fixative. If desired, store at 4°C). A few drops of cells were dropped from about 18 inches high onto an angled, humidified microscope slide. The cells on the slide were immediately spread by very gently blowing across the top of the slide. Slides were air dried at least 10 minutes (Slides are now stable for a long time). For centromere labeling, slides with metaphase spreads were denatured by immersion at 72 °C in 70% formamide / 2 x SSC (300 mM of Sodium Chloride, 30 mM of Sodium Citrate, PH 7.0 with 1N HCl) for 2 min then in 70% ethanol for 2 min in ice. Slides were again ethanol-dehydrated and

dried and then 10-12 µl of a pan-centromeric probe (Open Biosystems #SFP3336) were applied and covered with an 18 x 18 mm coverslip. Slides were hybridized for 16 hours at 37 °C in a humidified box, then washed in 2 x SSC for 5 min at 37°C. Slides were washed three times with 0.5 x SSC / 0.3% NP- 40 for 3 min at 37 °C, 2 x SSC / 0.1% NP-40 for 5 min at 22 °C, and finally in 2 x SSC for 5 min at 22 °C. 15 µL of Vectashield Mounting Media with 4', 6-diamidino-2-phenylindole (DAPI) (1.5 µg / ml) was used in each well for chromosomes staining, the coverslips were adhered to the slides using clear nail polish. All washes were performed in 50-ml glass Coplin jars. Slides were examined using 100 x objective of a Zeiss LSM510 Meta confocal microscope imaging system in Imaging Core Facility. The Core Facility is granted in part by NIH Grant P30 CA16059. On this confocal microscope, a 405-nm diode laser with 405-nm blocking and 420-nm long pass emission filters was for DAPI, and a 543-nm helium laser with 543-nm blocking and 560-615-nm bandpass emission filters were used for Cy3. Acentric fragments and dicentric chromosomes then were scored.

2.4 Micronuclei formation in interphase cells

Cells from SCAN1 patients and unaffected relatives were exposed to calicheamicin for 24 h, 4µg/ml of cytochalasin B (for blocking cytokinesis of cell cultures) also was added for 24 h before harvest to allow chromosomal damage to lead to the formation of micronuclei in bi- or multinucleated interphase cells. Cells were trypsinized and spun down at 800g for 6 minutes. Cell pellets were resuspended gently. For hypotonic treatment, 4 ml of 0.075 M KCl was added in each sample. After a 10 minute incubation at room temperature, cells were spun down again and fixed with cool Carnoy's fixative (methanol: acetic acid; 3:1) for 15 minutes at room temperature (disperse cells before the addition of fixative). The fixative procedure was repeated three times. The cell suspensions were dropped on wet slides previously cleaned with ethanol.

The slides were air-dried and stained with Giemsa dye (from Sigma), micronuclei were counted under a light microscope after complete wash.

2.5 Clonogenic survival assays of immortal mouse Tdp1 cells

Mouse Tdp1 knockout, Tdp1 double knockout (Tdp1-/-, Artemis -/-), Tdp1 wild type cells, and Artemis knockout cells were irradiated (MDS Nordion Gammacell 40 research irradiator (ON, Canada), with a ^{137}Cs source delivering a dose rate of 1.05 Gy/min) with 1.5 Gy or 3.0 Gy. 30 minutes after exposure, cells were trypsinized and centrifuged cell pellets were washed with PBS once, then 500 – 2000 cells from different samples were inoculated into 100-mm dishes in fresh RPMI1640 medium at 37°C. After 12 days incubation without any moving, cells were fixed with 100% methanol and stained with 1% of crystal violet, rinsed with water and air-dried, the colonies were counted manually.

2.6 Proliferation of Tdp1 MEFs

Wild type Tdp1 and *Tdp1*-Knockout mouse embryo fibroblasts (MEFs, littermates) were generated from Dr. Windle's lab in the Department of Human Genetics at VCU. These cells were cultured regularly in DMEM containing 10% heat inactivated fetal bovine serum (FBS, from Atlanta biologicals), 10,000 Units/ml penicillin and 10,000 µg/ml streptomycin, and in 5% CO_2 plus 3% or 20% oxygen, the percentage of oxygen was adjusted using an oxygen sensor and regulator and nitrogen source in a culture chamber. 25-cm^2 flasks were used for cell growth. Cells were cultured normally in 3% oxygen with other standard culture conditions before the experiment began. When these cells were cultured to 90% confluence, 1.7 X 10^5 cells were subcultured in 25-cm^2 flasks in both 20% and 3% oxygen for each sample. Concentration of each culture was checked and continued to passage 1.7 x 10^5 cells into a new 25-cm^2 every 4-6 days

(about 1 population doubling). If the number of cells did not reach to 1.7 $X10^5$ cells in some samples (such as Tdp1 knockout MEFs in 20% oxygen), all available cells in each culture would be taken for subculture. Cells were monitored for growth for 91 days. The growth curves were made by days against the log value of number of cells.

2.7 Growth assay of Tdp1 MEFs in 3% and 20% oxygen

Tdp1 wild type and Tdp1 knockout mouse embryo fibroblasts (MEFs, littermates) were cultured regularly in DMEM containing 10% heat inactivated fetal bovine serum (FBS, from Atlanta biologicals), 10,000 Units/ml penicillin and 10,000 µg/ml streptomycin, and in 5% CO2 plus 3% or 20% oxygen, the percentage of oxygen was adjusted using an oxygen sensor and regulator and nitrogen source in a culture chamber. For a cell growth assay, 0.5 $X10^5$ cells / per culture were seeded in a 6-well plate in completed DMEM, the concentration of viable cells was measured every three days for 15 days.

2.8 Flow cytometric assay

2.8.1 Determination of H2AX foci formation. MEFs were cultured in 20% and 3% oxygen for three days before harvest. Then 10^6 cells / sample were trypsinized, pelleted and the pellets were washed once with PBS. Cell suspensions were centrifuged and resuspended in 3 ml PBS. Cells were then fixed by dripping into 7 ml of cold 100% EtOH while vortexing. Then cells were left at 4°C overnight. Cells were resuspended in 1 ml of blocking reagent (5% FBS/PBS, freshly made), then cells were pelleted by spinning 5 minutes at 4000 rpm. Cells were resuspended in 500 µl of γ-H2AX monoclonal antibody (Anti-phospho-Histone H2A.X (Ser 139), 1:2500 dilution, from Millipore, #05-636) for 1 hour 30 minutes at room temperature. Cells were pelleted by spinning 5 min at 4000 rpm and washed twice with 1ml of 5% FBS/PBS/0.1% Triton

X-100. Then cells were suspended in 500 µl of secondary antibody with fluorescent tag (Alexa Fluor 488, goat anti-mouse IgG_1, 1:5000 dilution in 5% FBS/PBS, from Invitrogen) for 1 hour at room temperature. Cells were pelleted and washed 4 times with 5% FBS/PBS/0.1% Triton X-100. Cells were resuspended in 600 µl 5% FBS/PBS solution. The data were acquired using BD FACS 500 Scaliber flow cytometer and analyzed using FACS analysis software.

2.8.2 **Determination of cell cycle distribution**. MEFs were cultured in 20% and 3% oxygen for three days before harvest. Then 10^6 cells / sample were trypsinized, pelleted and the pellets were washed once with PBS. Cell suspensions were centrifuged and resuspended in 3 ml PBS. Cells were then fixed by dripping into 7 ml of cold 100% EtOH while vortexing. Then cells were left at 4°C until use (at least overnight). Cells were then pelleted and washed twice with 5% FBS/PBS to remove all ethanol which may interfere with propidium iodide (PI) staining. Cells were centrifuged and the pellet was resuspended in 200 µl of 0.5% FBS/PBS. To this cell suspension, 5 µl of RNase A (10 mg/ml, from Sigma) and 10 µl of propidium iodide (1 mg/ml, from Fisher) were added followed by incubation for 30 min at room temperature. The cells were pelleted and resuspended in 0.6 ml 0.5% FBS/PBS. The data were acquired using BD FACS 500 Scaliber flow cytometer and analyzed using Modfit analysis software.

2.9 Alkaline comet assay

The Trevigen Comet Assay protocol in combination with Trevigen cometslides were utilized in this experiment. Tdp1 normal and deficient MEFs cultured at 20% and 3% oxygen (four samples in total) were prepared for this experiment. When cells grew close to 90% confluence, 50µl of cell suspensions at 1 $x10^5$ cells per ml were combined with 500 µl molten LMAgarose (0.5 Low-Melting Point Agarose , 50 ml PBS Ca++, Mg++ free) in 1:10 ratios at 37^0C. The slides were

subsequently placed flat at 4^0C in the dark for 10 minutes and immersed in prechilled Lysis Solution (Trevigen, Gaithersburg, MD) at 4^0C for 40 minutes. Afterwards, the slides were immersed in freshly prepared Alkaline Unwinding Solution (300mM NaOH, 1mM EDTA, pH > 13) for 40 minutes at room temperature in the dark. The slides were electrophoresed at 21 volts (1V/cm) for 30 minutes in Alkaline Electrophoresis Solution (300mM NaOH, 1mM EDTA). The slides were then immersed in dH2O for 2 periods of 5 minutes and in 70% ethanol for 5 minutes. The slides were dried at room temperature for 15 minutes. The slides were stained with 100µl of 4^0C chilled diluted SYBR® Green I (1ul SYBR® Green I, 10ml TE Buffer pH 7.5). The slides were analyzed by epifluorescence microscopy (SYBR Green I's maximum excitation and emission are respectively 494 nm/521 nm) at 40x magnifications. At least 50 comets were scored per sample with open-source CometScore software.

2.10 Statistics

Error bars represent standard error of mean (SEM) for at least three independent experiments. Unpaired two tailed t-tests were performed and the data was reported as significant for P values <0.05.

III. RESULTS

3.1 Radiosensitivity of SCAN1 cells

In order to assess the role of TDP1 on 3′-PG processing in intact cells, SCAN1 cells and normal control cells were irradiated with different doses. Our previous studies have demonstrated that there is a severe deficit in 3′-PG processing in both whole-cell extracts and nuclear extracts of SCAN1 cells. If 3′-PG processing is absent in SCAN1 cells *in vivo*, then SCAN1 cells should be more sensitive than normal cells to ionizing radiation, which was evaluated to induce around 50% breaks with 3′-PG termini (Henner et al., 1983). The preliminary data suggested that SCAN1 cells were no more sensitive than normal cells to a single dose of ionizing radiation.

In order to evaluate the effect of ionizing radiation on SCAN1 cells, an alternative method, called dose fractionation was used since DSB repair by non-homologous end-joining is primarily responsible for split-dose recovery (Whitemore et al., 1989), this means that dose fractionation allows normal cells to repair damaged DNA during time intervals, whereas cells with DNA repair deficiencies will cycle into a more sensitive phase between treatments, rendering them more susceptible to radiation damage. So dose fractionation accentuates the radiosensitizing effects of repair deficiencies.

Two cell lines from SCAN1 patients and two cell lines from unaffected relatives were cultured until they reached plateau-phase cells. Then these cells were irradiated with different doses daily for five days (dose fractionation), and a growth assay was then performed by checking the cell numbers for all the samples once every other day for total 19 days. The growth curves indicated that cell lines from two SCAN1 patients were reproducibly mildly radiosensitive than normal controls. For example, at 5 x 0.8 Gy, a significant growth difference appeared around 6 days

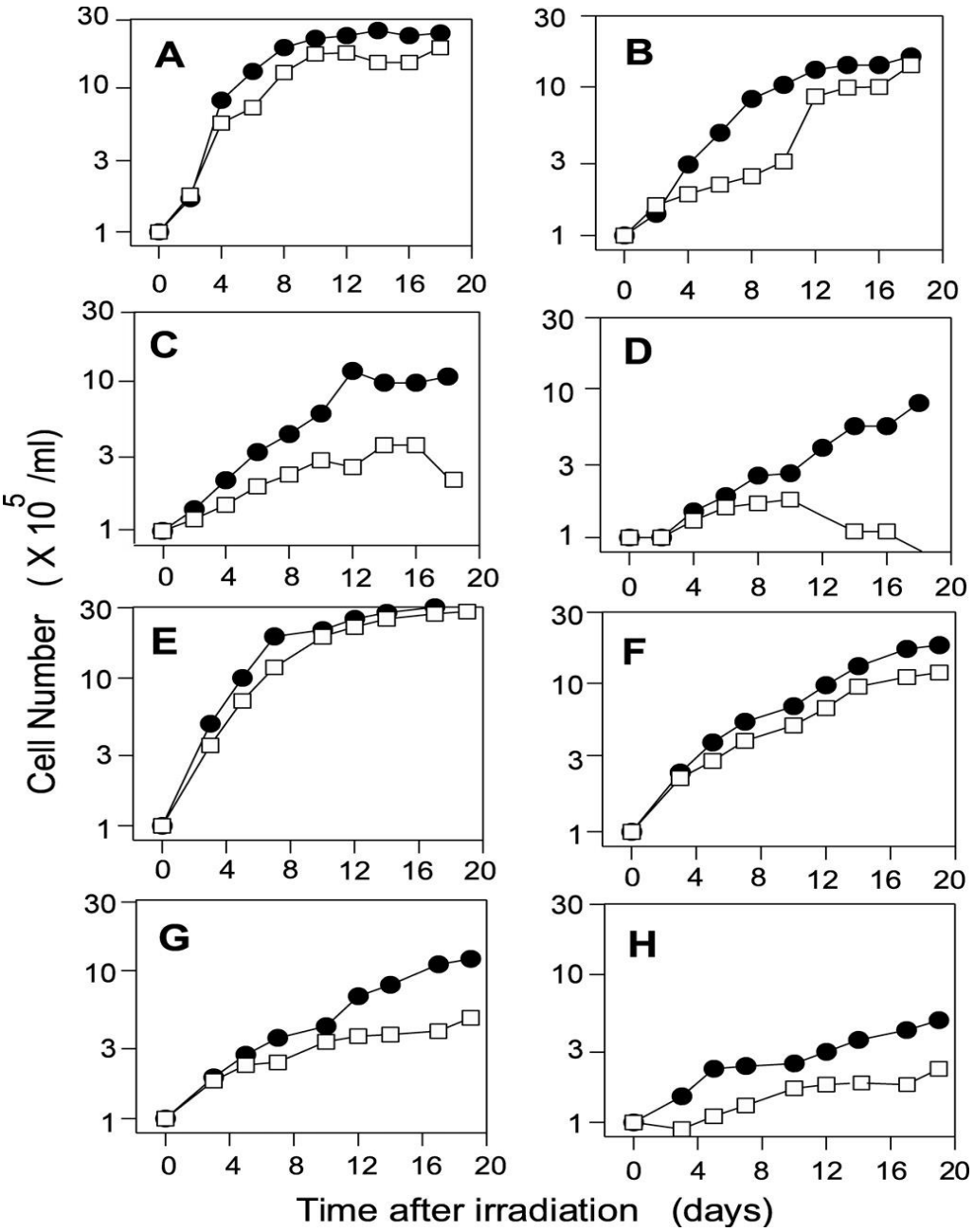

Figure 3-1. Radiosensitivity of SCAN1 cells. Plateau-phase normal cells (closed circles) or SCAN1 cells (open squares) were irradiated daily for 5 days with 0 (A), 0.4 (B), 0.8 (C) or 1.6 (D) Gy of γ-rays, then diluted to 10^5/ml for assessment of cell growth. (E–H) Identical experiment with another normal and another SCAN1 cell line.

after dose fractionation treatment. The most significant data was observed at the sample of 5 × 1.6 Gy (Figure 3-1D), showing that growth of normal cells resumed at 10 days after radiation, however, the SCAN1 cells had begun to die off at the same time. Moreover, by comparing growth of SCAN1 cells in 5 x 0.8 Gy (Figure 3-1C) with normal cells in 5 x 1.6 Gy (Figure 3-1D), the similar concentrations between them indicated that the SCAN1 cells were double sensitive to radiation, similar situation can also be observed in another SCAN1 cell line in Figure 3-1G and another normal cell line in Figure 3-1H. Furthermore, the SCAN1 cells in Figure 3-1 A-D showed a little bit more radiosensitivity than SCAN1 cell line used in Figure 3-1E – H. All this data coming together suggested that even though the radiosensitivity of SCAN1 cells is slightly higher than normal cells, this difference is reproducible, thus is believable.

There is another problem which should be noticed in this experiment, that is the low cloning efficiency of SCAN1 cells. When we tried to assess the radiosensitivity of SCAN1 cells, we typically performed a colongenic survival assay by using either agar cloning or limiting dilution assays (because SCAN1 and normal control cells need to be cultured in suspension), we failed to get reproducible survival data from any of these cell lines, mostly because of the low cloning efficiency (close to 1%). We shifted to growth assay to assess the radiosensitivity of SCAN1 cells. Although the simpler growth assays may overlook some small differences in radiosensitivity, and the present results did not distinguish between growth delay and cell killing, they do show a difference between two SCAN1 cell lines and normal cell lines in their response to radiation. Our previous experiments *in vitro* suggested that addition of recombinant TDP1 to SCAN1 whole cell and nuclear extracts restored 3′-PG removal and allowed subsequent gap filling on the aligned DSB ends. An idea raised for future work is to generate a mouse model harbering the SCAN1-equivalent mutant allele of TDP1, to assess their response to radiation.

3.2 TDP1-mutant SCAN1 cells show chromosomal hypersensitivity to calicheamicin

As mentioned before, Calicheamicins are a class of enediyne antibiotics derived from the bacterium Micromonospora echinospora, and calicheamicin γ1 is the most notable one. Activated calicheamicin forms a diradical species that simultaneously attacks both strands of DNA (Dedon et al., 1992). One end of each calicheamicin-induced DSB has a 5′-phosphate, and 3-base 3′ overhang with a 3′-phosphate. The opposite DSB end has a 5′ aldehyde and a 2-base 3′ overhang with either a 3′-phosphate or a 3′-PG (Figure 3-4A). Thus, the calicheamicin-induced DSBs that bear 3′-PG termini are similar to the synthetic substrates that require TDP1 for processing in cell extracts. Our previous experiments have demonstrated a role for TDP1 in repair of these DSBs *in vitro*, as well as the interplay between TDP1 and core end-joining proteins: *in vitro* experiment, affinity-tagged TDP1 which was overexpressed in human cells and purified, showed its effect on processing of various of 3′-PG DSB termini. Ku and DNA-PKcs inhibited TDP1-mediated processing of 3′-PG DSB termini, and ATP was capable of abrogating DNA-PK-mediated inhibition. Moreover, inhibition of DNA-PK blocks most but not all TDP1-mediated end processing in cell extracts.

In order to determine the possible role of TDP1 in repair of DSBs in intact cells, TDP1-mutant SCAN1 lymphoblastoid cells were treated with calicheamicin, and the formation of micronuclei was assayed (Figure 3-4B). Addition of 1 mM caffeine in each duplicate sample was to minimize arrest of cells in G2. The data in Figure 3-4B showed that the fraction of cells containing derived from unaffected relatives. Similarly, the data in Figure 3-4C indicated that levels of acentric chromosome fragments as measured on metaphase spreads with fluorescent-stained micronuclei was about 1.5-fold higher for SCAN1 cells than for identically treated normal cells

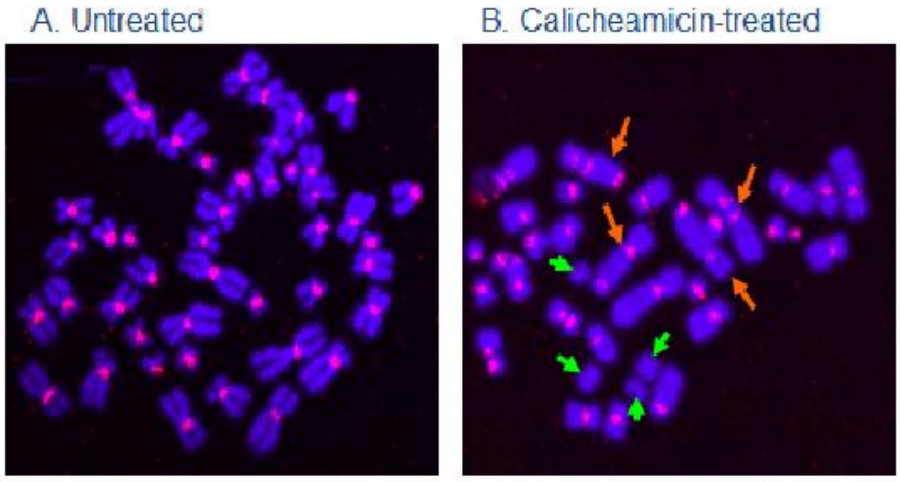

Figure 3-2. Metaphase spreads of untreated (A) or calicheamicin-treated (B) SCAN1 cells. Centromeres were labeled by hybridization to a Cy3-conjugated fluorescent probe. Cells in (B) treated with 6 pM calicheamicin for 24 hr show 4 dicentrics (orange arrows) and 4 acentric fragments (green arrowheads) (from Zhou & Povirk et al., 2009).

Methods: Following calicheamicin treatment, cells were incubated in the presence of 1 µg /ml colchicine for 1 hr, washed with PBS and swollen in 0.075 M KCl for 10 min, then centrifuged and fixed with 3:1 methanol/acetic acid. Following two washes in methanol/acetic acid, cells were dropped onto slides and dried at room temperature. Slides were dehydrated by immersion for 2 min each in 70%, 90% and 100% ethanol, then baked at 65°C for 15 min, washed in acetone for 10 min and dried. Slides were treated with 100 mg/ml RNase A in 2 X SSC under a parafilm coverslip for 1 hr at 37 °C in a humidified box, then washed for 5 min in 2 x SSC and for 10 min in PBS, dehydrated with an ethanol series and allowed to dry. Chromosomes were denatured by immersion in 70% formamide / 2 x SSC (adjusted to pH7 with HCl) for 2 min at 72 °C and then in 70% ethanol for 2 min in ice. Slides were again ethanol-dehydrated and dried and then 10-12 µl of a pan-centromeric probe (Open Biosystems) were applied and covered with an 18 x 18-mm coverslip. Slides were hybridized for 16 hr at 37°C in a humidified box, then washed in 2 x SSC for 5 min at 37°C, three changes of 0.5 x SSC / 0.3% NP-40 for 3 min at 37°C, 2 x SSC / 0.1% NP-40 for 5 min at 22 °C, and finally in 2 x SSC for 5 min at 22°C. The drained wet slides were counterstained with Vectashield containing DAPI (Vector Laboratories) under a coverslip that was sealed with clear lacquer. Slides were then coded and submitted for chromosome scoring as described. All washes were performed in 50-ml glass Coplin jars.

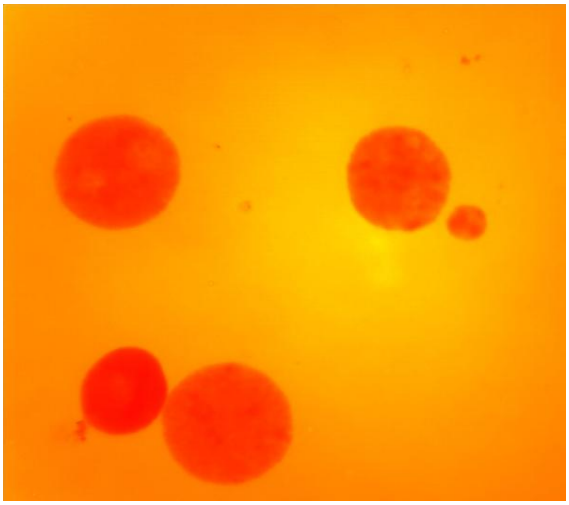

Figure 3-3. Micronucleus Formation. Cells from SCAN1 patients and unaffected relatives were exposed to calicheamicin for 24 hr. 4µg/ml of cytochalasin B (for blocking cytokinesis cell cultures) also was added for 24 h before harvest to allow chromosomal damage to lead to the formation of micronuclei in bi- or multinucleated interphase cells. Cells were trypsinized and centrifuged at 800g for 6 minutes. Cell pellets were resuspended gently. For hypotonic treatment, 4 ml of 0.075 M KCl were added to each sample. After a 10 minute incubation at room temperature, cells were centrifuged and fixed with cool Carnoy's fixative (methanol: acetic acid; 3:1) for 15 minutes at room temperature (disperse cells before the addition of fixative). The fixation step was repeated three times. Cell suspensions were dropped on wet slides previously cleaned with ethanol. The slides were air-dried and stained with Giemsa dye (from Sigma), and micronuclei were counted under a light microscope after complete wash.

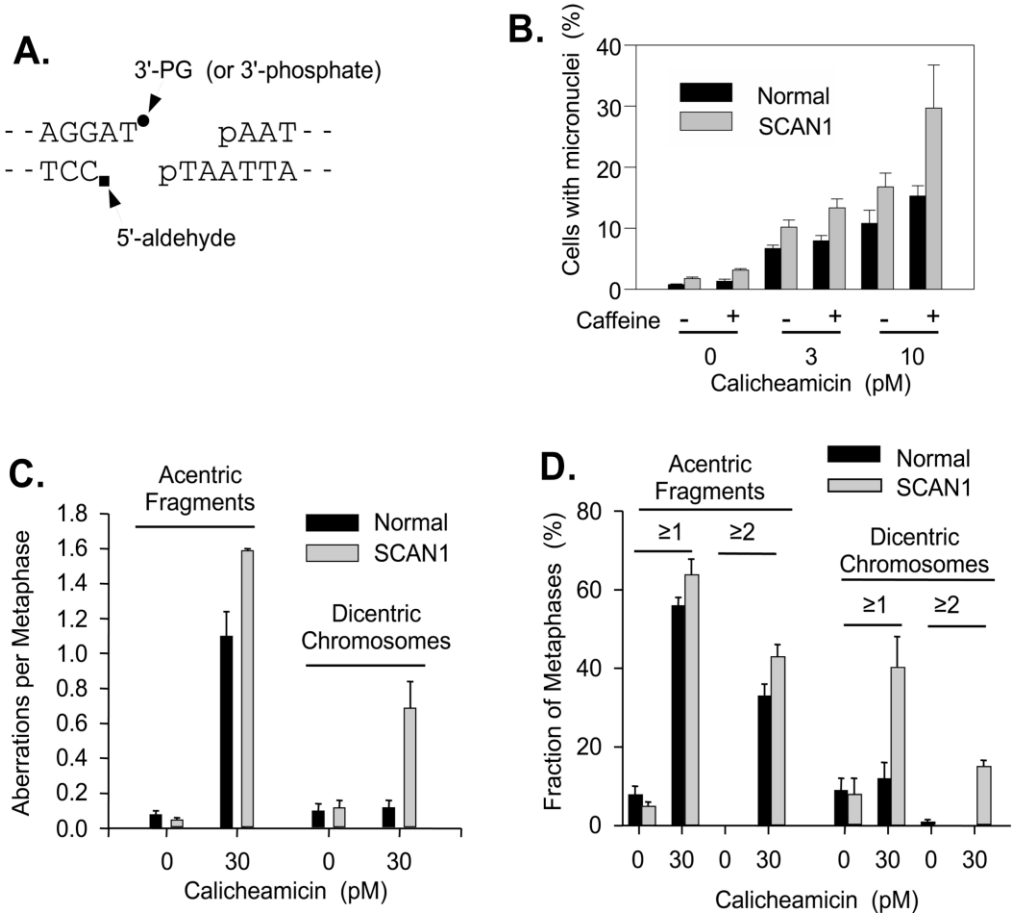

Figure 3-4. Chromosomal sensitivity of SCAN1 cells to calicheamicin. A. Structure of calicheamicin-induced DSBs: one end of each calicheamicin-induced DSB has a 5′-phosphate, and 3-base 3′ overhang with a 3′-phosphate. The opposite DSB end has a 5′ aldehyde and a 2-base 3′ overhang with either a 3′-phosphate or a 3′-PG. B. SCAN1 or normal cells were treated with the indicated concentrations of calicheamicin and then stained with DAPI, and the fraction of cells with micronuclei was determined. Approximately 100 cells were scored in each of three independent experiments (student test, SCAN1 vs. normal: fraction of cells with micronuclei with 3 pM calicheamicin without caffeine, $p = 0.06$, with caffeine, $p = 0.07$; 10 pM calicheamicin without caffeine, $p = 0.14$, with caffeine, $p = 0.11$). C. Following calicheamicin treatment, metaphase cells were collected for 1 hr with colchicine, and then metaphase spreads were prepared and hybridized with a fluorescent (Cy3) centromeric probe. Approximately 50 metaphases were photographed and scored for acentric fragments and dicentric chromosomes, and the number of each type of aberration per cell was calculated (student test, SCAN1 vs. normal: Acentric fragments with 30 pM calicheamicin, $p = 0.02$; Dicentric chromosomes with 30 pM calicheamicin, $p = 0.03$). D. Same data as (C.), but expressed as the fraction of cells having at least one, or more than one aberration of each type (student test, SCAN1 vs. normal: Acentric fragments ≥ 1, $p = 0.13$; ≥ 2, $p = 0.08$; Dicentric chromosomes ≥ 1, $p = 0.03$). The mitotic index was between 2% and 4% for all samples.

(Figure 3-4B). Furthermore, the number of dicentric chromosomes was much greater in SCAN1 than in normal cells, and there was a particularly dramatic increase in the number of cells having more than one dicentric (Figure 3-4D). Elevated levels of calicheamicin-induced dicentric chromosomes were detected consistently in two other SCAN1 lines as well. While micronuclei and acentrics suggest chromosome breaks, dicentrics indicate chromosome misrepair. These results suggest that calicheamicin-induced DSBs were repaired less accurately and perhaps less efficiently or more slowly in SCAN1 cells than in normal cells.

Next, in order to assess the chromosomal sensitivity of TDP1 cells to ionizing radiation, normal or SCAN1 cell lines were treated with 1.5 Gy or 3 Gy of ionizing radiation and incubated for 16 hours, and caffeine (1 mM) was added at the same time in each dose to abrogate G2 arrest of cells which could potentially bias the results by delaying mitosis of more heavily damaged cells. Then dicentric chromosomes were scored. The data showed, addition of caffeine in both normal or SCAN1 cell lines without radiation treatment produced small fraction of metaphases with dicentrics in both normal and SCAN1 cell lines, and SCAN1cells have slightly high fraction of metaphases with dicentrics than normal cells; in both cell lines treated with 1.5 Gy or 3 Gy and without caffeine addition, SCAN1 cells have a slightly high fraction of metaphases with dicentrics than normal cells. However, addition of caffeine declined difference between two cell lines in 1.5 Gy samples, and normal cells in 3 Gy sample even has slightly high fraction of metaphases with dicentrics than SCAN1 cells. Taken together, the data suggested that there was little if any chromosomal hypersensitivity to ionizing radiation (Figure 3-5).

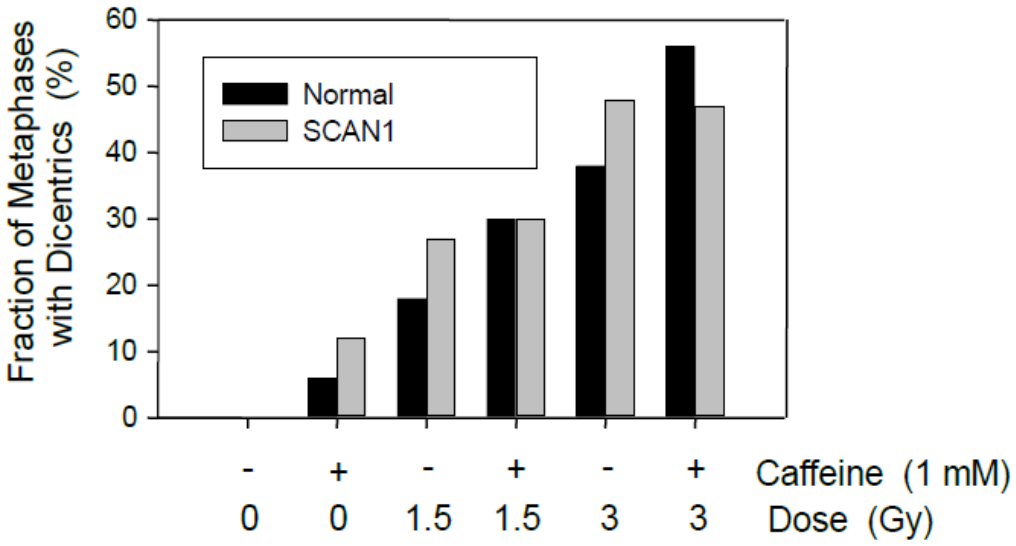

Figure 3-5. SCAN1 cell lines lack chromosomal sensitivity to ionizing radiation. Normal and SCAN1 cell lines were treated with 1.5 Gy or 3 Gy of ionizing radiation and incubated for 16 hr. Dicentric chromosomes were then scored.

3.3 Oxidative Stress Caused Poor Cell Proliferation in Early-passage Tdp-deficient MEFs

When we assessed the radiosensitivities of immortal Tdp1 mouse cells, we found that was little if any difference between Tdp1 normal and Tdp1 deficient cells (Figure 3-6). We thought that may be caused by the possible occurrence of a mutagenic or adaptive event in MEFs after long-term growth in 20% oxygen. Some studies suggested that MEFs senesce as a result of oxidative stress, and that MEFs senesce in culture in 20% oxygen but not in 3% oxygen, and the senescence was not due to telomere shortening (Parrinello et al., 2003). In addition, it was reported that survival curves were possible with early passage MEFs, but the resulting colonies were microcolonies (10-20 cells) and they were formed only in 3% oxygen not in 20% oxygen (Parrinello et al., 2003). So we first cultured early passage of Tdp1-deficient MEFs at normal culture conditions, including 20% oxygen, and found that Tdp1-deficient MEFs did not form colonies even in 3% oxygen and grew very poorly in 20% oxygen. In order to assess a role of oxidative stress on Tdp1 deficient MEFs, Tdp1 normal and Tdp1 deficient MEFs were cultured in 20% and 3% oxygen and the growth was assessed for up to 2 weeks. The growth assay started with the concentration of 5 $x10^4$ cells/ml in each sample in both 3% and 20% oxygen, then the concentrations of viable cells were examined every 3 days. The data suggested that Tdp1-deficient MEFs grew very slowly in both 20% and 3% oxygen, and the Tdp1-deficient MEFs grown in 20% oxygen showed a constantly, significant increased growth arrest compared to those in 3% oxygen. In contrast with this, Tdp1 normal MEFs in both 20% and 3% oxygen showed a rapid growth before both of them entered the plateau phase, the Tdp1 normal MEFs showed slightly delayed growth in 20% oxygen compared to those in 3% oxygen. A Tdp1 and Sod2 double-knockout MEF cell line was also involved in this growth assay in both oxygen conditions, this cell line also showed a constantly, but increased growth arrest in 20% oxygen

compared to the same MEFs in 3% oxygen. Since Sod2 was a well-known antioxidant, Sod2 deficient cells should exhibit a hypersensitivity to oxidative damage. But in our experiment, Sod2 did not exhibit any apparent effect as an antioxidant as Sod2-/-Tdp1-/- MEFs should the same severely compromised growth in both 3% and 20% oxygen as did Sod2+/+ Tdp1-/- MEFs. Although the simpler growth assays may overlook some small differences in response to oxidative stress, and the growth curves cannot distinguish between growth delay and cell killing, Tdp1-deficient MEFs do show an apparent growth arrest compared to Tdp1 normal MEFs in both 20% and 3% oxygen; moreover, Tdp1- deficient MEFs also showed a significantly increased growth arrest in response to oxidative stress. One thing need to be mentioned here is that all the MEFs cell lines used in this experiment were from different parental mouse lines, simply because that they were the only available Tdp1 MEFs cell lines at the time when the experiments were performed. In order to avoid the effects of genetic differences between MEF cultures other than Tdp1 status, littermate Tdp1+/+ and Tdp1-/- MEFs were acquired at a later time, the above experiments were repeated and the results are reported in the next section.

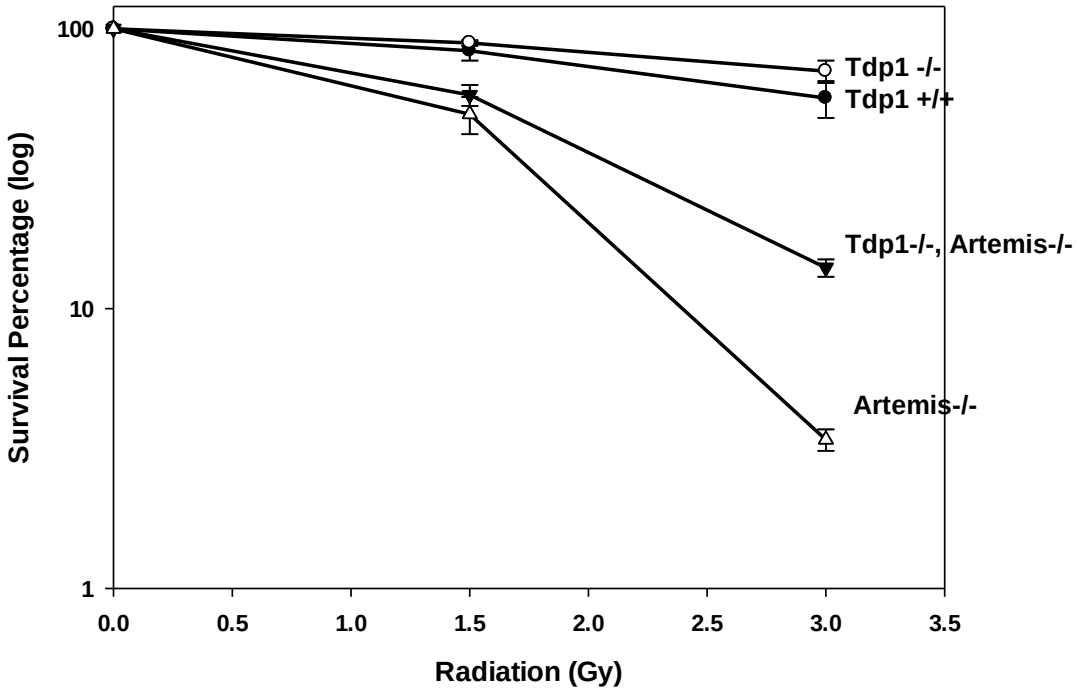

Figure 3-6. Immortal mouse Tdp1 cells lack sensitivity to ionizing radiation. Tdp1- deficient MEFs, Tdp1 and Artemis double knockout MEFs, Artemis-deficient cells, and Tdp1 normal MEFs were treated with 1.5 Gy or 3.0 Gy. 30 minutes after exposure, 500 and 2000 cells were inoculated in 10-cm dishes for each dose with fresh RPMI 1640 medium at 37°C. After 12 days incubation without any moving, cells were fixed with 100% methanol and stained with 1% of crystal violet, the colonies were counted manually. Error bars indicate SEM for two independent experiments.

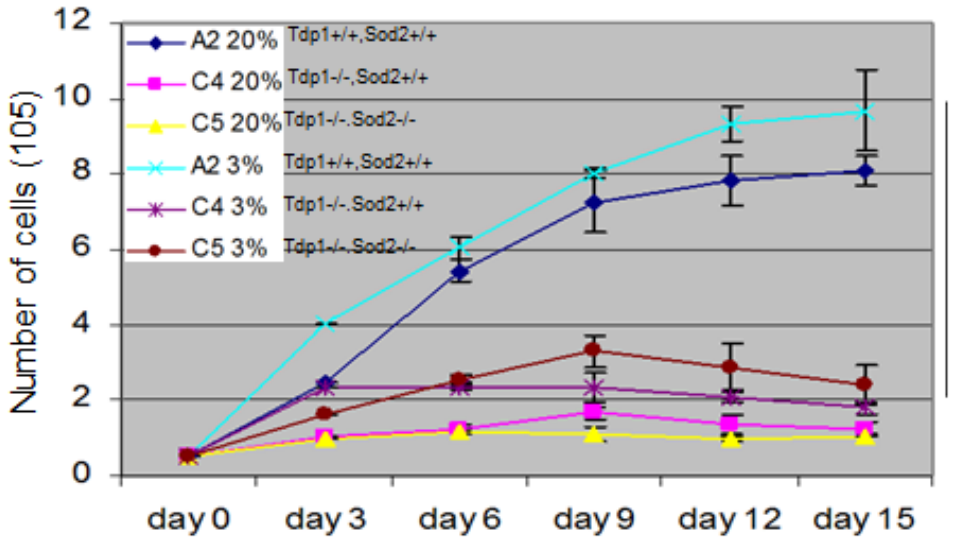

Figure 3-7. Growth Assay of Tdp1-deficient MEFs in 20% and 3% Oxygen. Three MEF cell lines were examined in both 20% and 3% oxygen. The experiment started with 5 x 10^4 cells/ml in each 25 cm^2 flask at day 0, and the concentration was examined for each sample once every 3 days, for total 15 days. Error bars represent SEM for three independent experiments.

3.4 Oxidative stress enhances cellular replicative arrest in Tdp1-deficient MEFs

It is believed that MEFs senesce as a result of oxidative stress (Parrinello et al., 2003). In order to assess how oxidative stress affects cell proliferation in Tdp1 deficient MEFs, the phenotypes of Tdp1 normal and deficient MEFs were compared from every early passage, in both 20% oxygen, which is atmospheric oxygen, and 3% oxygen, which is physiological oxygen (Figure 3-8). What we expect to see is that (Todaro et al., 1963), in 20% oxygen, normal MEFs cells grow well for the first 1-2 weeks (2-4 population doublings) before cells' proliferation starts to become slower. After 5-6 weeks (10-12 population doublings), the cells senesce with no change in cell number for more than 1 week. Then proliferation eventually recovers due to outgrowth of immortal variants (Todaro et al., 1963). In our experiment, two Tdp1 normal MEF cell lines and two Tdp1 deficient MEF cell lines were monitored for more than 100 days. We found that Tdp1-normal cells grew faster in 3% oxygen and were able to sustain rapid growth, and did not show signs of senescence, whereas the same cell lines cultured in 20% oxygen gave a slow and delayed growth until approximately day 50, At that point, proliferation in one of the cell lines accelerated to a rate matching that of cells in 3% oxygen, presumably due to some form of adaptation to 20% oxygen. Tdp1-deficient MEFs in 3% oxygen showed extremely slow growth until around day 60 when they began to grow, but still more slowly than normal cells. Whereas in 20% oxygen, Tdp1-deficient MEFs showed no net growth until around day 80, when they eventually began to grow. In early passages, these cultures appeared to contain many dead and dying cells, suggesting that proliferation was approximately balanced by cell death.

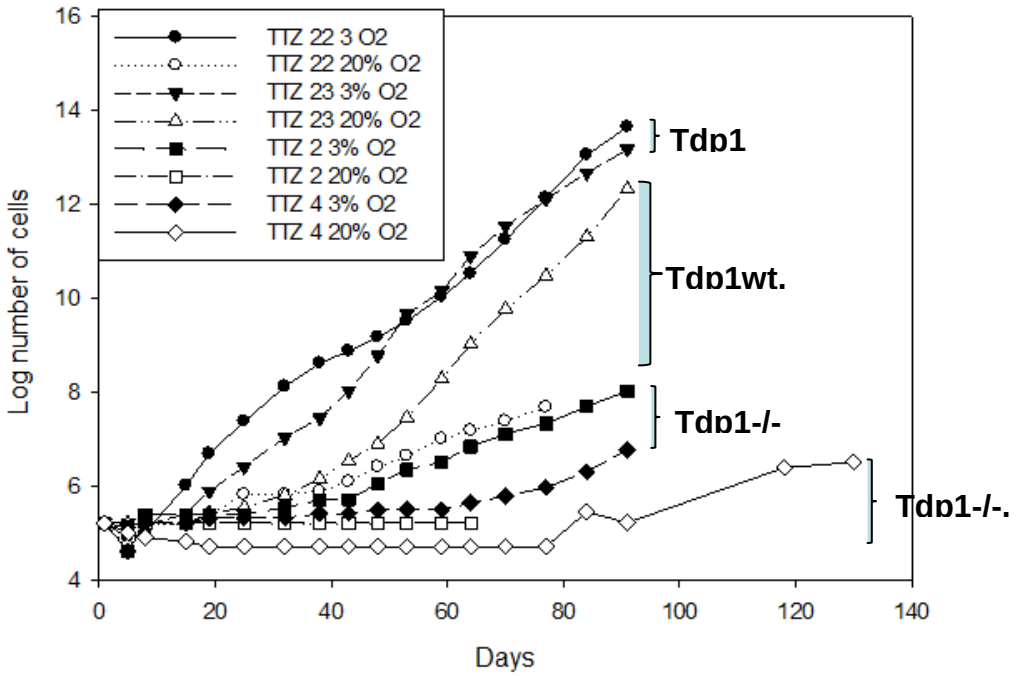

Figure 3-8. Cell proliferation assays of Tdp1 normal and deficient MEFs in early passage in 20% and 3% oxygen. Two Tdp1 deficient MEF cell lines (TTZ 2 & TTZ 4) and two Tdp1 normal MEFs cell lines (TTZ 22 and TTZ 23) in early passage were examined. Cells were cultured normally in 3% oxygen with other standard culture conditions before the experiment began. When these cells were cultured to 90% confluence, 1.7 X 10^5 cells were subcultured in 25-cm^2 flasks in both 20% and 3% oxygen for each sample. Concentration of each culture was checked and continued to passage 1.7 x 10^5 cells into a new 25-cm^2 every 4-6 days (about 1 population doubling). If the number of cells did not reach to 1.7 X10^5 cells in some samples (such as Tdp1 knockout MEFs in 20% oxygen), all available cells in each culture would be taken for subculture. Cells were monitored for growth for 91 days. The growth curves were made by days against the log value of number of cells.

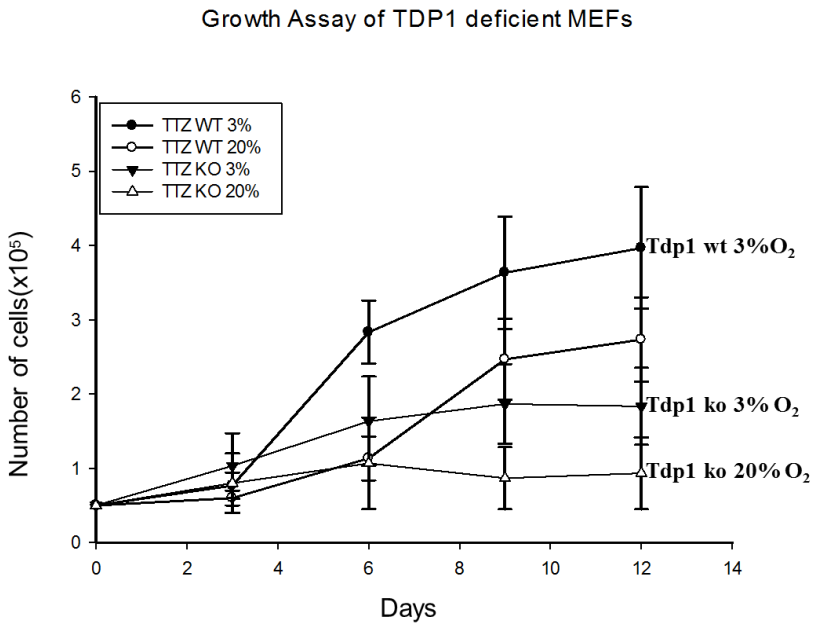

Figure 3-9. Growth assay of early passage Tdp1-deficient MEFs in 20% and 3% oxygen. Tdp1 normal MEFs and Tdp1-deficient MEFs were examined. The experiment started with 5 x 10^4 cells /ml in each sample at day 0, the concentration was examined once every 3 days, for total 12 days. Each curve was made from 3 individual experiments, the error bars showed standard deviations.

A growth assay also was performed for Tdp1 normal and deficient MEFs in both 20% and 3% oxygen (Figure 3-9). All the procedures were same with what were done in Section 3.3**.** Tdp1 normal and deficient MEFs from littermate embryos were examined in both 20% and 3% oxygen. The data showed that Tdp1-deficient MEFs exhibited significant growth arrest in 3% oxygen, and even worse in 20% oxygen. Tdp1 normal MEFs showed a mild growth arrest in 20% oxygen compared to the same cell line in 3% oxygen. All these data suggested an effect of oxidative stress on Tdp1-deficient MEFs.

Taken together, we concluded from these data that oxidative stress arrests the growth of normal early passage MEFs which are capable of overcoming this growth arrest and eventually resuming growth in 20% oxygen. Tdp1 deficient MEFs grew poorly in 3% oxygen, and even worse in 20% oxygen. Tdp1 deficient MEFs need much longer time to adapt to ambient 20% oxygen and resume growth.

3.5 Tdp1 MEFs Showed Cell Cycle Arrest in G2 Phase

Oxidative stress and resulting DNA damage have effects on cell cycle regulation, and the cell has developed numerous mechanisms to ensure correct cell division. Cell cycle checkpoints are control mechanisms to verify whether the processes at each phase of the cell cycle have been accurately completed before entering into the next phase. A very important function of checkpoints is to assess DNA damage by utilizing the same sensor-signal-effector mechanism. G1 checkpoint is located at the end of the cell cycle G1 phase, right before entry into S phase, making the decision of whether the cell should divide, delay division, or enter a resting stage. In animal cells, the G1 phase checkpoint (also called restriction point) is controlled mainly by action of the CKI- p16 (CDK- p16). CDK 4/6, cyclin D1, Rb, E2F transcription factor, as well as

cyclin E and CDK2 are involved in G1- S phase transition. Activation of Intra S phase checkpoint by DNA damage initiates an ATM-Chk2-Cdc25A-CDK2-CyclinA-Cdc45 pathway to slow down ongoing DNA synthesis to allow possible DNA repair before entering into G2 phase (Falck et al., 2001; Mailand et al., 2000; Costanzo et al., 2000). G2 checkpoint is located at the end of G2 phase, right before the mitotic phase. The CDKs associated with this checkpoint are activated by phosphorylation of the CDK through Maturation Promoting Factor (MPF). DNA damage occurs frequently prior to mitosis. In order to prevent transmission of this damage to daughter cells, the cell cycle is arrested through inactivation of the Cdc25 phosphatase by the ATM kinase protein which phosphorylates Cdc25 which leads to its ubiquitinylation and destruction.

In order to examine how oxidative stress affects cell cycle in Tdp1-deficient MEFs, a flow cytometric assay was performed with Tdp1 normal and deficient MEFs. A Tdp1-normal and a Tdp1-deficient MEF culture were shifted to 20% oxygen from 3% oxygen 72 hour before the cells were fixed for preparation of flow cytometric assay. The data indicated that Tdp1-deficient MEFs showed an apparent G2 arrest in both 20% and 3% oxygen, and Tdp1-deficient MEFs in 20% have less population in G1 phase, Tdp1 normal MEFs showed a distribution typical of proliferating cells, with more cells in G1 than in G2, in both 20% and 3% oxygen (Figure 3-10). For both cell lines, G1 and G2 peaks were rather broad, probably due to variable cell size and morphology, making it difficult to accurately estimate G1, G2/M and S-phase populations. Nevertheless, it was evident that the absence of Tdp1 resulted in substantial cell cycle arrest at G2 phase, and that 20% oxygen caused a slightly higher fraction of the cell population to be blocked in G2 phase.

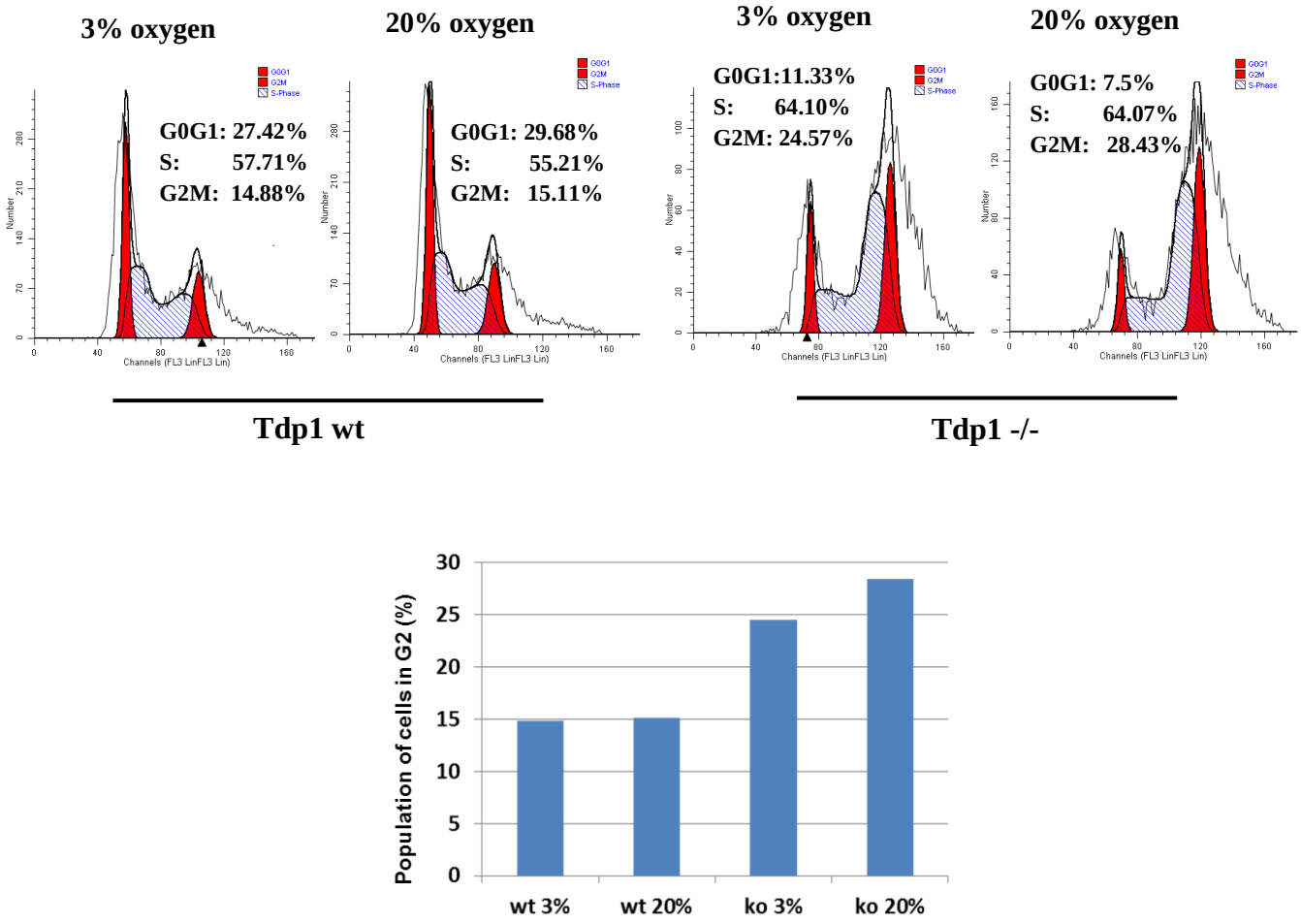

Figure 3-10. Flow Cytometric Assay of Cell Cycle Distribution in Tdp1 deficient MEFs. A Tdp1 normal and a Tdp1 deficient MEFs sample were shifted to 20% oxygen from 3% oxygen 72 hour before cells were fixed for preparation of flow cytometric assay. Modfit software was used for data analysis.

3.6 Tdp1-deficient MEFs accumulate higher levels of oxidative DNA damage.

Our experiments suggest that oxidative stress arrest the growth of Tdp1-deficient MEFs. The studies of proliferation and cytogenetic profiles of various DNA repair-deficient MEFs from other groups also indicated that MEFs accumulated more DNA damage in 20% oxygen than 3% oxygen, and the DNA damage limited MEFs proliferation in 20% oxygen (Parrinello et al., 2003). In order to examine if Tdp1 MEFs accumulate more damaged DNA in 20% oxygen, alkaline comet assays were performed with Tdp1 MEFs in 20% and 3% oxygen, to detect single and double stranded breaks (Figure 3-11). Tdp1 normal and deficient MEFs were cultured in 20% oxygen to allow enough time for production of DNA damage and repair. 50 µl of a cell suspension at 1 x 10^5 cells per milliliter were used for each sample. We found that Tdp1 deficient MEFs accumulated significantly more DNA damage compared to normal MEFs in both 20% oxygen and 3% oxygen, whereas Tdp1 deficient MEFs did not have significant more DNA damage in 20% than in 3% oxygen.

These results are consistent with the proposed role of oxidative stress in MEFs, suggesting that DNA damage induced by oxidative stress arrested the growth of MEFs in 20% oxygen, whereas Tdp1-deficient MEFs accumulated more DNA damage in 3% oxygen, and even more in 20% oxygen.

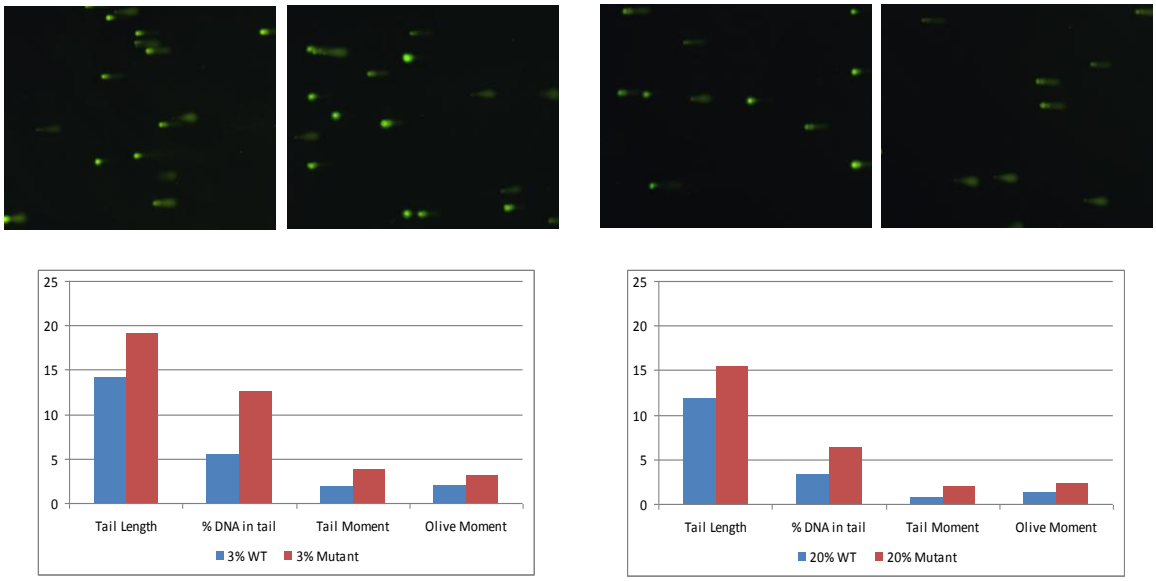

Figure 3-11. Measure of DNA damage by alkaline comet assay. Tdp1 normal and deficient MEFs cultured at 20% and 3% oxygen (4 samples in total) were prepared for this experiment. 50 µl of cell suspensions at 1 x10^5 cells per ml were combined with 500 µl molten LMAgarose in 1:10 ratios at 37^{0}C. The slides were subsequently placed flat at 4^{0}C in the dark for 10 minutes and immersed in prechilled Lysis Solution at 4^{0}C for 40 minutes. Afterwards, the slides were immersed in freshly prepared Alkaline Unwinding Solution for 40 minutes at room temperature in the dark. The slides were electrophoresed at 21 volts (1V/cm) for 30 minutes in Alkaline Electrophoresis Solution. The slides were then immersed in dH_2O for 2 periods of 5 minutes and in 70% ethanol for 5 minutes. The slides were dried at room temperature for 15 minutes. The slides were stained with 100µl of 4^{0}C chilled diluted SYBR® Green I. The slides were analyzed by epifluorescence microscopy at 40 x magnifications. 50 comets were scored per sample with open-source CometScore software.

IV. DISCUSSION

4.1 Radiosensitivity of SCAN1 Cells

When topoisomerase I fails to religate transient DNA strand breaks, an irreversible linkage between a tyrosyl residue of topoisomerase I and the 3′ DNA terminus is formed (Hsiang et al., 1989; Pommier et al., 1993); DNA DSBs induced by radiation and radiomimetic drugs, such as calicheamicin, typically bear 3′-PG and 3′-phosphate termini at the DNA ends. All these blocked 3′ termini must be converted to 3′-OH termini to allow ligation by DNA ligases and gap filling by DNA polymerases (Pouliot et al., 1999; Interthal et al., 2001). There are several 3′ terminal processing enzymes that could be candidates for such removal, such as Ape1, PNKP, and TDP1, as well as Dnase III, Mre 11 and Artemis. However, based on the known specificities of these enzymes, only TDP1 was implicated as being capable of acting on protruding 3′-PG termini of DSB ends. Ape1 worked only on blunt and recessed 3′ ends (Suh et al., 1997), PNKP mainly removed 3′-phosphate that was left from 3′-PG processing by TDP1 (Inamdar et al., 2002), and Artemis acted efficiently as endo/exonuclease only on longer 3′ overhangs (usually longer than four bases) (Ma et al., 2002; Moshous et al., 2001).

Our previous experiments have shown that there was no detectable PG termini processing on 3 base 3′ overhangs when model substrates are incubated in extracts of SCAN1 cells harboring mutant TDP1, suggesting that almost all processing of protruding 3′-PG termini is attributable to TDP1. However, the in vivo results from growth assays indicate only slight radiosensitivity in two SCAN1 cell lines, and only for cells in plateau phase subjected to fractionated radiation. These results suggest that most PG-terminated DSBs are still repaired in SCAN1 cells, but presumably by alternative pathway other than the TDP1-dependent pathway. For example,

Artemis is able to process 3′ overhangs longer than four bases, while blunt and recessed 3′-PG ends can be processed by Ape1. So we think the fraction of radiation-induced DSBs with a strict requirement for TDP1 may be very low, and we assume for these breaks, there may be alternative, or even more complicated repair pathways that can be triggered when classic NHEJ pathway fails, as suggested by the "repair foci" of DSB repair factors that can be detected long after the majority of DSBs have already been repaired (Bradbury et al., 2003). These repair complexes may be not available, or not functional in cell extracts, and this may be a possible cause for the complete lack of 3′-PG processing in extract-based assays. For the future work, we need to discover what factors can account for the apparent difference between the severe repair deficiency seen in extracts and the relatively mild radiosensitivity of SCAN1 cells.

Other studies of the functions and mechanism of TDP1 indicated that as a DNA repair protein, TDP1 is phosphorylated, and its phosphorylation is stimulated by ionizing radiation (Valerie et al., 2003; Goodarzi et al., 2003; Lees-Miller, 1996; Durocher et al., 2001). But phosphorylation is not required for the basic enzymatic function of TDP1 (H. Tatavarthi and L. F. Povirk, unpublished data). Nevertheless, phosphorylation could modulate TDP1 activity or influence its interactions with other repair proteins. These conclusions provided some evidence for possible involvement of TDP1 in repair pathways for radiation-induced DNA damage.

Other studies gave more insights to better understand the SCAN1 pathology. It is generally assumed that SCAN1 pathology is most possibly due to the failure of mutant TDP1 to efficiently repair topoisomerase I-associated DNA damage (Takashima et al., 2002). This repair deficiency could indirectly confer sensitivity to oxidative DNA damage, as certain oxidative lesions tend to promote formation of topoisomerase I cleavable complexes (Pourquier et al., 1999), which upon

replication can be converted to cytotoxic topoisomerase-terminated DSBs (Hsiang et al., 1989). Nevertheless, a role for PG-terminated DSBs in SCAN1 pathology cannot be excluded. Accumulation of sufficient DSBs in terminally differentiating neurons caused significant neurological pathology in the absence of DSB repair (Barnes et al., 1998; Gao et al., 1998). There is evidence that some 'spontaneous' DSBs reflect damage by oxygen free radicals associated with normal oxidative metabolism in mitochondria (Karanjawala et al., 2003). Futuremore, SCAN1 pathology is similar to that of both Friedreich ataxia and ataxia with oculomotor apraxia (AOA1) (Caldecott et al., 2003), both of which have been linked to oxidative damage. TDP1 deficiency confers sensitivity to ionizing radiation or to bleomycin, a radiomimetic drug that specifically induces PG-terminated DSBs (Liu et al., 2002). Thus, while the exact sequence of events culminating in the SCAN1 phenotype remains to be elucidated, several lines of circumstantial evidence suggest a possible linkage among TDP1 deficiency, oxidative damage, DSBs and cerebellar ataxia. Even though lymphoblastoid cell lines derived from SCAN1 patients show at most only mild radiosensitivity, it is possible that endogenous tissues of SCAN1 patients are more sensitive to free radical damage than the cell lines. Because cultured cells are subjected to higher oxygen tensions than would occur *in vivo*, they may be more likely to adapt to TDP1 deficiency, for example, by upregulating alternative pathways for repair of DSBs and other oxidative damage.

4.2 **TDP1-mutant SCAN1 Cells Show Chromosomal Hypersensitivity to Calicheamicin**

TDP1 has been implicated in repair of topoisomerase I-mediated SSBs and DSBs since TDP1-mutant SCAN1 cells, and extracts from these cells are deficient in rejoining of SSBs induced by topoI inhibitors (Katyal et al., 2007, Khamisy et al., 2005). TDP1 directly binds to DNA ligase

III, which is a primary ligase in SSB repair pathway (EI-Khamisy et al., 2005). TDP1 can also process 3′-PG termini typically induced by free radical species. Extracts from SCAN1 cells and Tdp1-/- murine fibroblasts are completely deficient in processing of protruding 3′-PG DNA DSB ends (Zhou et al., 2005; Hawkins et al., 2009). All these results suggested a possible role for TDP1 in resolving 3′ blocks at DSB termini. However, either SCAN1 cells or Tdp1-/- mouse fibroblasts did not showed any apparent DSB repair defect in a direct assays for repair of radiation-induced DSBs in intact cells (EI-Khamisy et al., 2007; Katyal et al., 2007). The explanation for this result is complicated by disparate measurements of the frequency of 3′-PG termini at these DSB ends. Early studies indicated that around 50% radiation-induced DNA breaks had 3′-PG termini (Henner et al., 1983), however, a more recent study reported that the frequency of 3′-PG termini at these DSB ends evaluated by mass spectrometry was as low as 10% (Chen et al., 2007). If 10% is close to the correct value, then our result was easy to understand, since 3′-PG processing defect for lesions with such a low frequency might not produce significant radiosensitivity.

Our laboratory has also examined the interplay between TDP1 and core NHEJ proteins Ku and DNA-PK at DNA DSB ends. Ku and DNA-PK exist with a high levels in human cells (Anderson et al., 1992), and our own data suggested that when purified Ku and unphosphorylated DNA-PKcs bound to a DNA end bearing a 3′-PG overhang, the PG can be completely protected from TDP1-mediated glycolate removal (Zhou et al., 2009). Phosphorylation of the 2609-2647 serine/threonine cluster in DNA-PKcs has been proposed to induce a conformational change that promotes end accessibility (Reddy et al., 2004). Addition of ATP strongly promoted 3′-PG processing, suggesting that DNA-PK-mediated phosphorylation does make the end more accessible. Moreover, there are other DNA-PK-catalyzed phosphorylation sites that are at least

as important as the 2609-2647 cluster in promoting end accessibility and processing. However, there remains some controversy over whether this accessibility reflects dissociation of DNA-PKcs from ends or only a conformational change in DNA-PKcs that still remains bound. To address this question, a recent study from our laboratory employed DNase footprinting on the theory that if DNA-PKcs remains bound with a conformational change, a qualitatively different footprint might result. The results suggested a fraction of the DNA ends was free of any DNA-PK, while the rest remained fully sequestered. There are at least 12 potential sites of autophosphorylation on DNA-PKcs, and extensive autophosphorylation of DNA end-bound DNA-PKcs can result in complete dissociation from the DNA ends (Chan et al., 1996). In our experiments, DNA-PKcs is present in at least a 10-fold excess with respect to DNA ends, and thus any dissociated phosphorylated DNA-PKcs would likely be replaced by a fresh unphosphorylated DNA-PKcs molecule. Moreover, the experiments in nuclear extracts showed that PG removal proceeded continuously from the beginning of reaction, even with high concentrations of DNA-PKcs and Ku, and that there is significant PG removal in the first 5 min even when DNA-PK kinase activity is blocked. These results suggested that end sequestration by DNA-PKcs is not immediate and that there is opportunity for end processing before the end-bound repair complex is fully formed.

In intact cells, the chromosomal sensitivity of SCAN1 cells to calicheamicin provides additional evidence of a role for TDP1 in DSB repair. The calicheamicin-induced DSB is unique in that one end of the break often bears a 3′-PG and a 5′-aldehyde (Dedon et al., 1992; Povirk, 1996); thus, at least one of these blocking groups must be removed in order for end joining to proceed. Most free radical-mediated DSBs resulting from deoxyribose oxidation at positions other than C-4′ will bear 5′-phosphate and 3′-phosphate termini (Hutchinson et al., 1985; Ward et al., 1988), and

the latter can be readily converted to 3′-hydroxyls by PNKP, which binds to the core NHEJ protein XRCC4. Thus, the vast majority of DSBs induced by diffusible free radicals could presumably be rejoined in at least one strand without any additional enzymes for removal of modified ends. The presence of abnormal termini in both strands at one end of the calicheamicin-induced DSB may explain, in part, the extraordinary cytotoxicity of this compound, as well as the apparent requirement for TDP1 for optimal repair. These doubly blocked ends are likely to be resistant to many of the 3′→5′ and 5′→3′ exonucleases that otherwise might initiate resection-based end joining (Harrigan et al., 2007). Their resolution may instead require either a specific end-processing enzyme such as TDP1, or an endonucleolytic cleavage near the terminus, perhaps preceded by limited helicase-mediated unwinding of the terminal base pairs.

Thus, taken together, the results suggest that despite lack of demonstrable specific interactions with core NHEJ proteins, TDP1 can participate in resolution of blocked 3′ DSB termini in the context of NHEJ. Although Artemis nuclease plus DNA-PK can also process blocked termini on 3′ overhangs, this processing is slow and inefficient for very short overhangs (Povirk et al., 2007). Therefore, in SCAN1 cells, 3′-PG-terminated DSBs may tend to persist longer than in normal cells, potentially increasing the probability that they will be incorrectly joined. The very small enhancement of calicheamicin cytotoxicity seen in TDP1-knockdown cells, as well as the finding that in SCAN1 cells calicheamicin-induced dicentrics are enhanced more than chromosome breaks, suggest that TDP1 deficiency confers a marked increase in misrepair but perhaps only a slight defect in the extent of overall rejoining.

4.3 Oxidative Stress Enhances Growth Arrest in Tdp1 deficient MEFs

Most mammalian cells cannot proliferate indefinitely due to a process called replicative senescence. Human cells undergo replicative senescence largely because of telomere shortening, but MEFs senesce predominantly as a result of oxidative stress (Parrinello et al., 2003). Our result indicated that Tdp1 normal MEFs grew faster and did not show signs of senescence in 3% oxygen, compared to same cell line cultured in 20% oxygen which showed a delayed growth. This result was consistent with previous reports from other groups (Todaro et al., 1963; Parrinello et al., 2003). Furthermore, some studies found that, despite a lack of change in cell number at senescence, some MEFs synthesized DNA, possibly reflecting endoreduplication or unscheduled DNA synthesis (Parrnello et al., 2003). Senescence in MEFs can be induced by treating MEFs with hydrogen peroxide, a strong oxidant. Senescent MEFs developed an alternative morphology and expressed β-galactosidase (Chen et al., 2001). Our data also showed that Tdp1 deficient MEFs exhibited an apparent growth arrest in 3% oxygen that was even more severe in 20% oxygen, indicating that oxidative stress, combined with the absence of the DNA repair enzyme Tdp1 might cause the growth arrest of MEFs. Studies from other groups elucidated this phenomenon with cytogenetic analysis, they found that MEFs cultured in 20% oxygen accumulated two fold more chromosomal breaks than MEFs cultured in 3% oxygen, and absence of a DNA repair enzyme in MEFs increased the frequency of chromosome fragments in 3% oxygen and even more in 20% oxygen (Goytisolo et al., 2001). The comet assay is a primary method to measure oxidative DNA damage (Mckelvey-Martin et al., 1993), and a preliminary study in cooperation with another member in our lab has indicated that Tdp1-deficient MEFs accumulated more DNA damage than normal MEFs. Moreover, Formation of H2AX foci indicates occurrence of DSB, as phosphorylated H2AX (Gamma-H2AX) is a sensitive target for

looking at DSBs in cells. We have an ongoing experiment to check the H2AX foci formation in Tdp1-deficient MEFs by Flow Cytometric Assay.

When we assessed the radiosensitivities of immortal Tdp1 mouse cells, we found that there was no detectable difference between Tdp1-normal and Tdp1-deficient cells. We thought that this could be caused by the possible occurrence of a mutagenic or adaptive event in MEFs in 20% oxygen. Studies from other groups proved that immortal MEFs cultured in 20% oxygen have substantial DNA damage, and that immortalization of MEFs is usually caused by mutations in p53 or p19 ^{ARF} (Kamijo et al., 1997), these adaptive changes do not prevent DNA damage, but rather render cells insensitive to it (Kamijo et al., Parrinello et al., 2003).

Overall, we have shown that Tdp1 deficiency results in severe growth arrest in MEFs, that is at least partially dependent on oxidative stress.

4.4 Tdp1 Deficient MEFs Showed Cell Cycle Arrest in G2 Phase

Cell cycle checkpoints are control mechanisms that monitor successful completion of early cell cycle events and the integrity of the cell and generate delays in cell cycle progression in response to DNA damage (Hartwell et al., 1989; Kastan et al., 1997; Elledge et al., 1996). Cell cycle checkpoints operate in all phases of the cell cycle. Our data indicated that Tdp1 deficient MEFs showed an apparent G2 arrest in both 20% and 3% oxygen, compared to Tdp1 normal MEFs, which showed a normal cell cycle distribution in both 20% and 3% oxygen (Figure 3-5), suggesting that some Tdp1 deficient cells cannot further enter M phase of cell cycle until the damaged DNA were repaired. DSBs are potent triggers of cell cycle arrest and apoptosis. Single strands breaks can become double strand breaks after replication by collapse of replication forks. So, DSBs in Tdp1 deficient MEFs formed during replication would accumulate in G2 phase and

induced G2 arrest in both 20% and 3% oxygen. Tdp1 deficient MEFs in 20% oxygen may accumulate more damage in G2 phase. So we think that deficiency of Tdp1 is the key factor for the induction of G2 arrest, not oxygen related. Deficiency of Tdp1 in MEFs causes failure of some DSBs to repair. These DSBs may occur in G1 phase, S phase, or G2 phase. Usually, cells exposed to DNA damaging agents, such as oxidative stress, in early G1 phase may arrest at the point in mid G1 phase, whereas those in late G1 or S phase will delay the DNA synthesis. Those exposed in early to mid G2 may arrest in mid G2, whereas those in late G2 or early M phase will arrest in mitosis (Shackelford et al., 1999). Studies from other groups have outlined the mechanisms by which damaged DSBs activate G2 cell cycle checkpoint. The regulatory linkage between ATR and Chk1 strongly implicates ATR as a proximal component of the DNA damage-induced G2 checkpoint in mammalian cells (Zhang et al., 2006). DNA damage leads to the activation of Chk1, which, in turn, phosphorylates the Cdc25C, a mitosis-promoting phosphatase. Phosphorylation of Cdc25C then promotes its binding with 14-3-3 proteins, which prevents its activation of the mitotic cyclin B-Cdc2 kinase, and damaged cells are effectively blocked from entering mitosis (Zhang et al., 2006). ATM also contributes to the inhibition of Cdc25C activity, particularly in IR-damaged cells, by activating Chk2, which is able to phosphorylate Cdc25C in vitro (Brown et al., 1999). In cells that express both ATM and ATR, ATM may activate Chk2 to reinforce the block to cyclin B-Cdc2 activation imposed by the ATR-hChk1 pathway. ATM is essential for G2 checkpoint activation after cells have traversed G1 and S phase (Zhang et al., 2006).

V. Conclusions and Further Perspectives

Even though previous studies in our group have demonstrated that there is a severe deficit in 3′-PG processing in both whole-cell extract and nuclear extracts of SCAN1 cells, we found in this

study that SCAN1 cells were only mildly radiosensitive compared to normal control cells. These results suggested that most PG-terminated DSBs are still repaired in SCAN1 cells, but presumably by an alternative pathway that is not TDP1-dependent. Artemis has been found to process 3′ PG-terminated overhangs longer than four bases, while blunt and recessed 3′-PG ends can be processed by Ape1. We assume there may be alternative, or even more complicated repair pathways that can be triggered when classic NHEJ pathway fails, as suggested by the "repair foci" of DSB repair factors that can be detected long after the majority of DSBs have already been repaired (Bradbury et al., 2003). For the future work, we need to further define the reason for the apparent difference between the severe repair deficiency seen in extracts and the relatively mild radiosensitivity of SCAN1 cells occurred. Our previous experiments *in vitro* suggested that addition of recombinant TDP1 to SCAN1 whole cell and nuclear extracts restored 3′-PG removal and allowed subsequent gap filing on the aligned DSB ends, in future we plan to generate a normal TDP1-complemented SCAN1 mouse model, to assess their response to ionizing radiation.

In the study of the effect of oxidative stress on cellular proliferation in Tdp1-deficient MEFs, we found that Tdp1-normal MEFs grew faster and did not show signs of senescence in 3% oxygen, compared to same cell line cultured in 20% oxygen which showed a delayed growth and an obvious proliferative arrest. This result was consistent with previous reports from other groups (Todaro et al., 1963; Parrinello et al., 2003). Furthermore, our data also showed that early-passage Tdp1-deficient MEFs grew poorly in 3% oxygen and even worse in 20% oxygen. Comet assays also showed Tdp1-deficient MEFs accumulated more DNA breaks than normal control MEFs. These results are consistent with the hypothesis that oxidative stress produces severe cell cycle arrest and poor cell growth in Tdp1-deficient MEFs. Studies from other groups elucidated

this phenomenon with cytogenetic analysis, which suggested that MEFs cultured in 20% oxygen accumulated two fold more chromosomal breaks than MEFs cultured in 3% oxygen, and absence of a DNA repair enzyme in MEFs increased the frequency of chromosome fragments in 3% oxygen and even more in 20% oxygen (Goytisolo et al., 2001). Thus, we will examine chromosome aberrations in MEFs in both 3% and 20% cultures to prove our results in genomic level. The comet assay is a frequently used method to measure oxidative DNA damage (Mckelvey-Martin et al., 1993). Even though preliminary comet data (obtained with the help of Vijay Menon, another member of our laboratory) has indicated that Tdp1-deficient MEFs accumulated more DNA damage than normal MEFs, we need to determine whether there is a significant difference in DNA damage levels in Tdp1 MEFs between 20% oxygen and 3% oxygen. Since senescent MEFs can develop an alternative morphology and express β-galactosidase, we need to check the morphology and expression of β-galactosidase of Tdp1-deficient MEFs in different oxygen conditions. Gamma-H2AX is sensitive target for looking at DSBs in cells. We have an ongoing experiment to check the formation of gamma-H2AX in Tdp1 MEFs. Furthermore, we can try to measure the expression of $p19^{ARF}$ and p16, two growth-inhibitory tumor suppressors as well as p53 in early and later passages of Tdp1 deficient cells, to determine whether they enforce the observed arrest, and how arrest is eventually overcome in late-passage cells.

References

Ahnesorg, P., P. Smith and S. Jackson, 2006. XLF interacts with the XRCC4-DNA ligase IV complex to promote DNA nonhomologous end-joining. Cell, 124 (2): 301-313.

Anderson, C.W. and S.P. Lees Miller, 1992. The nuclear serine/threonine protein kinase DNA-PK. Crit. Rev. Eukaryot. Gene Expr., 2 (4): 283-314.

Andres, S., M. Modesti, C. Tsai, G. Chu and M. Junop, 2007. Crystal structure of human XLF: a twist in nonhomologous DNA end-joining. Mol. Cell, 28 (6): 1093-1101.

Aylon, Y., B. Liefshitz and M. Kupiec, 2004. The CDK regulates repair of double-strand breaks by homologous recombination during the cell cycle. EMBO J., 23 (24): 4868-4875.

Barthelmes, H., M. Habermeyer, M. Christensen, C. Mielke, H. Interthal, J. Pouliot, F. Boege and D. Marko, 2004. TDP1 overexpression in human cells counteracts DNA damage mediated by topoisomerases I and II. J. Biol. Chem., 279 (53): 55618-55625.

Baskar, R., S. Yap, K.L.M. Chua and K. Itahana, 2012. The diverse and complex roles of radiation on cancer treatment: therapeutic target and genome maintenance. American journal of cancer research, 2 (4): 372-382.

Ben Porath, I. and R. Weinberg, 2005. The signals and pathways activating cellular senescence. International journal of biochemistry cell biology, 37 (5): 961-976.

Bradbury, J.M. and S.P. Jackson, 2003. The complex matter of DNA double-strand break detection. Biochem. Soc. Trans., 31 (1): 40-44.

Branzei, D. and M. Foiani, 2007. Template Switching: From Replication Fork Repair to Genome Rearrangements. Cell, 131 (7): 1228-1230.

Brown, A.L., C.H. Lee, J.K. Schwarz, N. Mitiku, H. Piwnica Worms and J.H. Chung, 1999. A human Cds1-related kinase that functions downstream of ATM protein in the cellular response to DNA damage. Proc. Natl. Acad. Sci. U. S. A., 96 (7): 3745-3750.

Bryans, M., M.C. Valenzano and T.D. Stamato, 1999. Absence of DNA ligase IV protein in XR-1 cells: evidence for stabilization by XRCC4. Mutat. Res., 433 (1): 53-58.

Buck, D., L. Malivert, R. de-Chasseval, A. Barraud, O. Sanal, A. Plebani, M. Hufnagel, F. le-Deist, A. Fischer, A. Durandy, J. de Villartay and P. Revy, 2006. Cernunnos, a novel nonhomologous end-joining factor, is mutated in human immunodeficiency with microcephaly. Cell, 124 (2): 287-299.

Burnet, N.G., R. Wurm and J.H. Peacock, 1996. Low dose-rate fibroblast radiosensitivity and the prediction of patient response to radiotherapy. Int. J. Radiat. Biol., 70 (3): 289-300.

Busuttil, R., M. Rubio, M.E.T., J. Campisi and J. Vijg, 2003. Oxygen accelerates the accumulation of mutations during the senescence and immortalization of murine cells in culture. Aging cell, 2 (6): 287-294.

Cadenas, E., G. Merenyi and J. Lind, 1989. Pulse radiolysis study of the reactivity of Trolox C phenoxyl radical with superoxide anion. FEBS Lett., 253 (1-2): 235-238.

Caldecott, K., 2003. DNA single-strand break repair and spinocerebellar ataxia. Cell, 112 (1): 7-10.

Chan, D.W. and S.P. Lees Miller, 1996. The DNA-dependent protein kinase is inactivated by autophosphorylation of the catalytic subunit. J. Biol. Chem., 271 (15): 8936-8941.

Chen, B., X. Zhou, K. Taghizadeh, J. Chen, J. Stubbe and P. Dedon, 2007. GC/MS methods to quantify the 2-deoxypentos-4-ulose and 3'-phosphoglycolate pathways of 4' oxidation of 2-deoxyribose in DNA: application to DNA damage produced by gamma radiation and bleomycin. Chem. Res. Toxicol., 20 (11): 1701-1708.

Chen, Q.M., V.C. Tu and J. Liu, 2000. Measurements of hydrogen peroxide induced premature senescence: senescence-associated beta-galactosidase and DNA synthesis index in human diploid fibroblasts with down-regulated p53 or Rb. Biogerontology, 1 (4): 335-339.

Chen, S., K.V. Inamdar, P. Pfeiffer, E. Feldmann, M.F. Hannah, Y. Yu, J.W. Lee, T. Zhou, S.P. Lees Miller and L.F. Povirk, 2001. Accurate in vitro end joining of a DNA double strand break with partially cohesive 3'-overhangs and 3'-phosphoglycolate termini: effect of Ku on repair fidelity. J. Biol. Chem., 276 (26): 24323-24330.

Costanzo, V., K. Robertson, C.Y. Ying, E. Kim, E. Avvedimento, M. Gottesman, D. Grieco and J. Gautier, 2000. Reconstitution of an ATM-dependent checkpoint that inhibits chromosomal DNA replication following DNA damage. Mol. Cell, 6 (3): 649-659.

Critchlow, S.E., R.P. Bowater and S.P. Jackson, 1997. Mammalian DNA double-strand break repair protein XRCC4 interacts with DNA ligase IV. Current biology, 7 (8): 588-598.

Dannenberg, J.H., A. van Rossum, L. Schuijff and H. te Riele, 2000. Ablation of the retinoblastoma gene family deregulates G (1) control causing immortalization and increased cell turnover under growth-restricting conditions. Genes development, 14 (23): 3051-3064.

Davies, D., H. Interthal, J. Champoux and W.G.J. Hol, 2002. The crystal structure of human tyrosyl-DNA phosphodiesterase, Tdp1. Structure, 10 (2): 237-248.

De Bont, R. and N. van Larebeke, 2004. Endogenous DNA damage in humans: a review of quantitative data. Mutagenesis, 19 (3): 169-185.

Dedon, P.C. and I.H. Goldberg, 1992. Free-radical mechanisms involved in the formation of sequence-dependent bistranded DNA lesions by the antitumor antibiotics bleomycin, neocarzinostatin, and calicheamicin. Chem. Res. Toxicol., 5 (3): 311-332.

Demple, B. and L. Harrison, 1994. Repair of oxidative damage to DNA: enzymology and biology. Annu. Rev. Biochem., 63: 915-948.

Dexheimer, T. and Y. Pommier, 2008. DNA cleavage assay for the identification of topoisomerase I inhibitors. Nature protocols, 3 (11): 1736-1750.

Dirac, A.M.G. and R. Bernards, 2003. Reversal of senescence in mouse fibroblasts through lentiviral suppression of p53. J. Biol. Chem., 278 (14): 11731-11734.

Dunne Daly, C.F., 1999. Principles of radiotherapy and radiobiology. Semin. Oncol. Nurs., 15 (4): 250-259.

Durocher, D. and S.P. Jackson, 2001. DNA-PK, ATM and ATR as sensors of DNA damage: variations on a theme?. Curr. Opin. Cell Biol., 13 (2): 225-231.

El Khamisy, S., G. Saifi, M. Weinfeld, F. Johansson, T. Helleday, J. Lupski and K. Caldecott, 2005. Defective DNA single-strand break repair in spinocerebellar ataxia with axonal neuropathy-1. Nature, 434 (7029): 108-113.

Elledge, S.J., 1996. Cell cycle checkpoints: preventing an identity crisis. Science, 274 (5293): 1664-1672.

Falck, J., N. Mailand, R.G. Syljuasen, J. Bartek and J. Lukas, 2001. The ATM-Chk2-Cdc25A checkpoint pathway guards against radioresistant DNA synthesis. Nature, 410 (6830): 842-847.

Fang, Y., S. Yang and G. Wu, 2002. Free radicals, antioxidants, and nutrition. Nutrition, 18 (10): 872-879.

Gao, Y., Y. Sun, K.M. Frank, P. Dikkes, Y. Fujiwara, K.J. Seidl, J.M. Sekiguchi, G.A. Rathbun, W. Swat, J. Wang, R.T. Bronson, B.A. Malynn, M. Bryans, C. Zhu, J. Chaudhuri, L. Davidson, R. Ferrini, T. Stamato, S.H. Orkin, M.E. Greenberg and F.W. Alt, 1998. A critical role for DNA end-joining proteins in both lymphogenesis and neurogenesis. Cell, 95 (7): 891-902.

Giloni, L., M. Takeshita, F. Johnson, C. Iden and A.P. Grollman, 1981. Bleomycin-induced strand-scission of DNA. Mechanism of deoxyribose cleavage. J. Biol. Chem., 256 (16): 8608-8615.

Gold, L., 2001. mRNA display: Diversity matters during in vitro selection. Proceedings of the National Academy of Sciences, 98 (9): 4825-4826.

Goodarzi, A., W. Block and S. Lees Miller, 2003. The role of ATM and ATR in DNA damage-induced cell cycle control. Prog. Cell Cycle Res., 5: 393-411.

Goytisolo, F.A., E. Samper, S. Edmonson, G.E. Taccioli and M.A. Blasco, 2001. The absence of the dna-dependent protein kinase catalytic subunit in mice results in anaphase bridges and in increased telomeric fusions with normal telomere length and G-strand overhang. Mol. Cell. Biol., 21 (11): 3642-3651.

Gu, X.Y., R.A. Bennett and L.F. Povirk, 1996. End-joining of free radical-mediated DNA double-strand breaks in vitro is blocked by the kinase inhibitor wortmannin at a step preceding removal of damaged 3' termini. J. Biol. Chem., 271 (33): 19660-19663.

Guirouilh-Barbat, J., S. Huck, P. Bertrand, L. Pirzio, C. Desmaze, L. Sabatier and B.S. Lopez, 2004. Impact of the KU80 Pathway on NHEJ-Induced Genome Rearrangements in Mammalian Cells. Mol. Cell, 14 (5): 611-623.

Hagen, U., 1986. Current aspects on the radiation induced base damage in DNA. Radiat. Environ. Biophys., 25 (4): 261-271.

Hamilton, J., F. Sato, Z. Jin, B. Greenwald, T. Ito, Y. Mori, B. Paun, T. Kan, Y. Cheng, S. Wang, J. Yang, J. Abraham and S. Meltzer, 2006. Reprimo methylation is a potential biomarker of Barrett's-Associated esophageal neoplastic progression. Clinical cancer research, 12 (22): 6637-6642.

Hammarsten, O. and G. Chu, 1998. DNA-dependent protein kinase: DNA binding and activation in the absence of Ku. Proc. Natl. Acad. Sci. U. S. A., 95 (2): 525-530.

Hammarsten, O., L.G. DeFazio and G. Chu, 2000. Activation of DNA-dependent protein kinase by single-stranded DNA ends. J. Biol. Chem., 275 (3): 1541-1550.

Harrigan, J., J. Fan, J. Momand, F. Perrino, V. Bohr and D. Wilson, 2007. WRN exonuclease activity is blocked by DNA termini harboring 3' obstructive groups. Mech. Ageing Dev., 128 (3): 259-266.

Hartley, K.O., D. Gell, G.C. Smith, H. Zhang, N. Divecha, M.A. Connelly, A. Admon, S.P. Lees Miller, C.W. Anderson and S.P. Jackson, 1995. DNA-dependent protein kinase catalytic subunit: a relative of phosphatidylinositol 3-kinase and the ataxia telangiectasia gene product. Cell, 82 (5): 849-856.

Hartwell, L.H. and T.A. Weinert, 1989. Checkpoints: controls that ensure the order of cell cycle events. Science, 246 (4930): 629-634.

Hawkins, A., M. Subler, K. Akopiants, J. Wiley, S. Taylor, A. Rice, J. Windle, K. Valerie and L. Povirk, 2009. In vitro complementation of Tdp1 deficiency indicates a stabilized enzyme-DNA adduct from tyrosyl but not glycolate lesions as a consequence of the SCAN1 mutation. DNA repair, 8 (5): 654-663.

Helleday, T., J. Lo, D. van Gent and B. Engelward, 2007. DNA double-strand break repair: from mechanistic understanding to cancer treatment. DNA repair, 6 (7): 923-935.

Henner, W.D., S.M. Grunberg and W.A. Haseltine, 1983. Enzyme action at 3' termini of ionizing radiation-induced DNA strand breaks. J. Biol. Chem., 258 (24): 15198-15205.

Hsiang, Y.H., M.G. Lihou and L.F. Liu, 1989. Arrest of replication forks by drug-stabilized topoisomerase I-DNA cleavable complexes as a mechanism of cell killing by camptothecin. Cancer Res., 49 (18): 5077-5082.

Huang, Y., X. Zhang and H. Chen, 1999. Regulation of Phospholipase D Activity in Human Hepatocacinoma Cells by Protein Kinases and D-sphingosine. Sheng Wu Hua Xue Yu Sheng Wu Wu Li Xue Bao (Shanghai)., 31 (5): 572-576.

Huertas, P., F. Cortes-Ledesma, A.A. Sartori, A. Aguilera and S.P. Jackson, 2008. CDK targets Sae2 to control DNA-end resection and homologous recombination. Nature, 455 (7213): 689-692.

Hutchinson, F., 1985. Chemical changes induced in DNA by ionizing radiation. Prog. Nucleic Acid Res. Mol. Biol., 32: 115-154.

Hutchinson, F., 1966. The molecular basis for radiation effects on cells. Cancer Res., 26 (9): 2045-2052.

Ihrie, R., E. Reczek, J. Horner, L. Khachatrian, J. Sage, T. Jacks and L. Attardi, 2003. Perp is a mediator of p53-dependent apoptosis in diverse cell types. Current biology, 13 (22): 1985-1990.

Inamdar, K., J. Pouliot, T. Zhou, S. Lees Miller, A. Rasouli Nia and L. Povirk, 2002. Conversion of phosphoglycolate to phosphate termini on 3' overhangs of DNA double strand breaks by the human tyrosyl-DNA phosphodiesterase hTdp1. J. Biol. Chem., 277 (30): 27162-27168.

Interthal, H., J.J. Pouliot and J.J. Champoux, 2001. The tyrosyl-DNA phosphodiesterase Tdp1 is a member of the phospholipase D superfamily. Proc. Natl. Acad. Sci. U. S. A., 98 (21): 12009-12014.

Interthal, H., H. Chen, T. Kehl Fie, J. Zotzmann, J. Leppard and J. Champoux, 2005. SCAN1 mutant Tdp1 accumulates the enzyme--DNA intermediate and causes camptothecin hypersensitivity. EMBO J., 24 (12): 2224-2233.

Isildar, M., M.N. Schuchmann, D. Schulte Frohlinde and C. von Sonntag, 1981. gamma-Radiolysis of DNA in oxygenated aqueous solutions: alterations at the sugar moiety. International journal of radiation biology related studies in physics, chemistry medicine, 40 (4): 347-354.

Jovanovic, M. and W. Dynan, 2006. Terminal DNA structure and ATP influence binding parameters of the DNA-dependent protein kinase at an early step prior to DNA synapsis. Nucleic Acids Res., 34 (4): 1112-1120.

Kamijo, T., F. Zindy, M.F. Roussel, D.E. Quelle, J.R. Downing, R.A. Ashmun, G. Grosveld and C.J. Sherr, 1997. Tumor suppression at the mouse INK4a locus mediated by the alternative reading frame product p19ARF. Cell, 91 (5): 649-659.

Kanaar, R., J.H.J. Hoeijmakers and D.C. van Gent, 1998. Molecular mechanisms of DNA double-strand break repair. Trends Cell Biol., 8 (12): 483-489.

Karanjawala, Z., D. Hinton, E. Oh, C. Hsieh and M. Lieber, 2003. Developmental retinal apoptosis in Ku86-/- mice. DNA repair, 2 (12): 1429-1434.

Karanjawala, Z., C. Hsieh and M. Lieber, 2003. Overexpression of Cu/Zn superoxide dismutase is lethal for mice lacking double-strand break repair. DNA repair, 2 (3): 285-294.

Karran, P., 2000. DNA double strand break repair in mammalian cells. Current opinion in genetics development, 10 (2): 144-150.

Kastan, M.B., 1997. Checkpoint controls and cancer. Introduction. Cancer Surv., 29: 1-6.

Katyal, S., S. el Khamisy, H. Russell, Y. Li, L. Ju, K. Caldecott and P. McKinnon, 2007. TDP1 facilitates chromosomal single-strand break repair in neurons and is neuroprotective in vivo. EMBO J., 26 (22): 4720-4731.

Katyal, S., S. el Khamisy, H. Russell, Y. Li, L. Ju, K. Caldecott and P. McKinnon, 2007. TDP1 facilitates chromosomal single-strand break repair in neurons and is neuroprotective in vivo. EMBO J., 26 (22): 4720-4731.

Katyal, S. and P. McKinnon, 2007. DNA repair deficiency and neurodegeneration. Cell cycle, 6 (19): 2360-2365.

Kodama, Y., D. Pawel, N. Nakamura, D. Preston, T. Honda, M. Itoh, M. Nakano, K. Ohtaki, S. Funamoto and A.A. Awa, 2001. Stable chromosome aberrations in atomic bomb survivors: results from 25 years of investigation. Radiat. Res., 156 (4): 337-346.

Kulju, K.S. and J.M. Lehman, 1995. Increased p53 protein associated with aging in human diploid fibroblasts. Exp. Cell Res., 217 (2): 336-345.

Langer, J.A., A.S. Acharya and P.B. Moore, 1975. Characterization of the particles produced by exposure of ribosomal subunits to urea. Biochim. Biophys. Acta, 407 (3): 320-324.

Lau, E., C. Zhu, R. Abraham and W. Jiang, 2006. The functional role of Cdc6 in S-G2/M in mammalian cells. EMBO Rep., 7 (4): 425-430.

Lee, K.J., J. Huang, Y. Takeda and W.S. Dynan, 2000. DNA ligase IV and XRCC4 form a stable mixed tetramer that functions synergistically with other repair factors in a cell-free end-joining system. J. Biol. Chem., 275 (44): 34787-34796.

Lees Miller, S.P., 1996. The DNA-dependent protein kinase, DNA-PK: 10 years and no ends in sight. Biochemistry and cell biology, 74 (4): 503-512.

Li, X. and W. Heyer, 2008. Homologous recombination in DNA repair and DNA damage tolerance. Cell Res., 18 (1): 99-113.

Li, Z., T. Otevrel, Y. Gao, H.L. Cheng, B. Seed, T.D. Stamato, G.E. Taccioli and F.W. Alt, 1995. The XRCC4 gene encodes a novel protein involved in DNA double-strand break repair and V(D)J recombination. Cell, 83 (7): 1079-1089.

Liao, Z., L. Thibaut, A. Jobson and Y. Pommier, 2006. Inhibition of human tyrosyl-DNA phosphodiesterase by aminoglycoside antibiotics and ribosome inhibitors. Mol. Pharmacol., 70 (1): 366-372.

Lieber, M., 2008. The mechanism of human nonhomologous DNA end joining. J. Biol. Chem., 283 (1): 1-5.

Lieber, M., J. Gu, H. Lu, N. Shimazaki and A. Tsai, 2010. Nonhomologous DNA end joining (NHEJ) and chromosomal translocations in humans. Subcellular Biochemistry, 50: 279-296.

Liu, C., J. Pouliot and H. Nash, 2002. Repair of topoisomerase I covalent complexes in the absence of the tyrosyl-DNA phosphodiesterase Tdp1. Proc. Natl. Acad. Sci. U. S. A., 99 (23): 14970-14975.

Liu, L.F. and J.C. Wang, 1987. Supercoiling of the DNA template during transcription. Proceedings of the National Academy of Sciences, 84 (20): 7024-7027.

Liu, W., Y. Zhu, M. Guo, Y. Yu and G. Chen, 2007. Therapeutic efficacy of NSC606985, a novel camptothecin analog, in a mouse model of acute promyelocytic leukemia. Leuk. Res., 31 (11): 1565-1574.

Lodish, H., R. Rodriguez and D. Klionsky, 2004. Points of view: lectures: can't learn with them, can't learn without them. Cell biology education, 3 (4): 202-211.

Low, M.G. and P. Stutz, 1999. Inhibition of the plasma glycosylphosphatidylinositol-specific phospholipase D by synthetic analogs of lipid A and phosphatidic acid. Arch. Biochem. Biophys., 371 (2): 332-339.

Ma, Y., U. Pannicke, K. Schwarz and M. Lieber, 2002. Hairpin opening and overhang processing by an Artemis/DNA-dependent protein kinase complex in nonhomologous end joining and V(D)J recombination. Cell, 108 (6): 781-794.

Mahajan, K., S. Nick McElhinny, B. Mitchell and D. Ramsden, 2002. Association of DNA polymerase mu (pol mu) with Ku and ligase IV: role for pol mu in end-joining double-strand break repair. Mol. Cell. Biol., 22 (14): 5194-5202.

Mailand, N., J. Falck, C. Lukas, R.G. Syljuasen, M. Welcker, J. Bartek and J. Lukas, 2000. Rapid destruction of human Cdc25A in response to DNA damage. Science, 288 (5470): 1425-1429.

Meek, K., V. Dang and S. Lees Miller, 2008. DNA-PK: the means to justify the ends?. Adv. Immunol., 99: 33-58.

Metcalfe, S.M., C.E. Canman, J. Milner, R.E. Morris, S. Goldman and M.B. Kastan, 1997. Rapamycin and p53 act on different pathways to induce G1 arrest in mammalian cells. Oncogene, 15 (14): 1635-1642.

Miao, H., H. Liu, E. Navarro, P. Kussie and Z. Zhu, 2006. Development of heparanase inhibitors for anti-cancer therapy. Curr. Med. Chem., 13 (18): 2101-2111.

Mimori, T. and J.A. Hardin, 1986. Mechanism of interaction between Ku protein and DNA. J. Biol. Chem., 261 (22): 10375-10379.

Mohapatra, S., M. Kawahara, I.S. Khan, S.M. Yannone and L.F. Povirk, 2011. Restoration of G1 chemo/radioresistance and double-strand-break repair proficiency by wild-type but not endonuclease-deficient Artemis. Nucleic Acids Research, 39 (15): 6500-6510.

Moshous, D., I. Callebaut, R. de Chasseval, B. Corneo, M. Cavazzana Calvo, F. Le Deist, I. Tezcan, O. Sanal, Y. Bertrand, N. Philippe, A. Fischer and J.P. de Villartay, 2001. Artemis, a novel DNA double-strand break repair/V(D)J recombination protein, is mutated in human severe combined immune deficiency. Cell, 105 (2): 177-186.

Mozumder, A., 1985. Early production of radicals from charged particle tracks in water. Radiation research.Supplement, 8: S33-S39.

Muller, C., G. Rodrigo, P. Calsou and B. Salles, 1999. [DNA-dependent protein kinase: a major protein involved in the cellular response to ionizing radiation]. Bull. Cancer, 86 (12): 977-983.

Nakano, M., Y. Kodama, K. Ohtaki, M. Itoh, R. Delongchamp, A.A. Awa and N. Nakamura, 2001. Detection of stable chromosome aberrations by FISH in A-bomb survivors: comparison with previous solid Giemsa staining data on the same 230 individuals. Int. J. Radiat. Biol., 77 (9): 971-977.

Namekawa, M., Y. Takiyama, K. Sakoe, H. Shimazaki, M. Amaike, K. Niijima, I. Nakano and M. Nishizawa, 2001. A large Japanese SPG4 family with a novel insertion mutation of the SPG4 gene: a clinical and genetic study. J. Neurol. Sci., 185 (1): 63-68.

Narita, M., S. Nunez, E. Heard, A. Lin, S. Hearn, D. Spector, G. Hannon and S. Lowe, 2003. Rb-mediated heterochromatin formation and silencing of E2F target genes during cellular senescence. Cell, 113 (6): 703-716.

Nick McElhinny, S.A., C.M. Snowden, J. McCarville and D.A. Ramsden, 2000. Ku recruits the XRCC4-ligase IV complex to DNA ends. Mol. Cell. Biol., 20 (9): 2996-3003.

Nivens, M., T. Felder, A. Galloway, M.M.O. Pena, J. Pouliot and H.T. Spencer, 2004. Engineered resistance to camptothecin and antifolates by retroviral coexpression of tyrosyl DNA phosphodiesterase-I and thymidylate synthase. Cancer Chemother. Pharmacol., 53 (2): 107-115.

Ohtaki, K., Y. Kodama, M. Nakano, M. Itoh, A.A. Awa, J. Cologne and N. Nakamura, 2004. Human fetuses do not register chromosome damage inflicted by radiation exposure in lymphoid precursor cells except for a small but significant effect at low doses. Radiat. Res., 161 (4): 373-379.

Ouellette, M.M., M. Liao, B.S. Herbert, M. Johnson, S.E. Holt, H.S. Liss, J.W. Shay and W.E. Wright, 2000. Subsenescent telomere lengths in fibroblasts immortalized by limiting amounts of telomerase. J. Biol. Chem., 275 (14): 10072-10076.

Parrinello, S., E. Samper, A. Krtolica, J. Goldstein, S. Melov and J. Campisi, 2003. Oxygen sensitivity severely limits the replicative lifespan of murine fibroblasts. Nat. Cell Biol., 5 (8): 741-747.

Plo, I., Z. Liao, J. Barcelo, G. Kohlhagen, K. Caldecott, M. Weinfeld and Y. Pommier, 2003. Association of XRCC1 and tyrosyl DNA phosphodiesterase (Tdp1) for the repair of topoisomerase I-mediated DNA lesions. DNA repair, 2 (10): 1087-1100.

Pommier, Y., 1998. Diversity of DNA topoisomerases I and inhibitors. Biochimie, 80 (3): 255-270.

Pouliot, J.J., K.C. Yao, C.A. Robertson and H.A. Nash, 1999. Yeast gene for a Tyr-DNA phosphodiesterase that repairs topoisomerase I complexes. Science, 286 (5439): 552-555.

Pourquier, P. and Y. Pommier, 1998. [Topoisomerases I: new targets for the treatment of cancer and mechanisms of resistance]. Bull. Cancer, Spec No: 5-10.

Pourquier, P., L. Ueng, J. Fertala, D. Wang, H. Park, J.M. Essigmann, M. Bjornsti and Y. Pommier, 1999. Induction of Reversible Complexes between Eukaryotic DNA Topoisomerase I and DNA-containing Oxidative Base Damages: 7,8-DIHYDRO-8-OXOGUANINE AND 5-HYDROXYCYTOSINE. Journal of Biological Chemistry, 274 (13): 8516-8523.

Pourquier, P., J.L. Waltman, Y. Urasaki, N.A. Loktionova, A.E. Pegg, J.L. Nitiss and Y. Pommier, 2001. Topoisomerase I-mediated Cytotoxicity of N-Methyl-N′-nitro-N-nitrosoguanidine: Trapping of Topoisomerase I by the O6-Methylguanine. Cancer Research, 61 (1): 53-58.

Povirk, L.F., 1996. DNA damage and mutagenesis by radiomimetic DNA-cleaving agents: bleomycin, neocarzinostatin and other enediynes. Mutat. Res., 355 (1-2): 71-89.

Povirk, L., T. Zhou, R. Zhou, M. Cowan and S. Yannone, 2007. Processing of 3'-phosphoglycolate-terminated DNA double strand breaks by Artemis nuclease. J. Biol. Chem., 282 (6): 3547-3558.

Ramsden, D.A. and M. Gellert, 1998. Ku protein stimulates DNA end joining by mammalian DNA ligases: a direct role for Ku in repair of DNA double-strand breaks. EMBO J., 17 (2): 609-614.

Ray, H., K. Moreau, E. Dizin, I. Callebaut and N. Venezia, 2006. ACCA phosphopeptide recognition by the BRCT repeats of BRCA1. J. Mol. Biol., 359 (4): 973-982.

Raymond, A., B. Staker and A. Burgin, 2005. Substrate specificity of tyrosyl-DNA phosphodiesterase I (Tdp1). J. Biol. Chem., 280 (23): 22029-22035.

Reddy, Y.V.R., Q. Ding, S. Lees Miller, K. Meek and D. Ramsden, 2004. Non-homologous end joining requires that the DNA-PK complex undergo an autophosphorylation-dependent rearrangement at DNA ends. J. Biol. Chem., 279 (38): 39408-39413.

Roberts, S., N. Strande, M. Burkhalter, C. Strom, J. Havener, P. Hasty and D. Ramsden, 2010. Ku is a 5'-dRP/AP lyase that excises nucleotide damage near broken ends. Nature, 464 (7292): 1214-1217.

Rogakou, E.P., D.R. Pilch, A.H. Orr, V.S. Ivanova and W.M. Bonner, 1998. DNA double-stranded breaks induce histone H2AX phosphorylation on serine 139. J. Biol. Chem., 273 (10): 5858-5868.

Roth, D.B., T.N. Porter and J.H. Wilson, 1985. Mechanisms of nonhomologous recombination in mammalian cells. Mol. Cell. Biol., 5 (10): 2599-2607.

Rothkamm, K., I. Kruger, L. Thompson and M. Lobrich, 2003. Pathways of DNA double-strand break repair during the mammalian cell cycle. Mol. Cell. Biol., 23 (16): 5706-5715.

Sage, J., G.J. Mulligan, L.D. Attardi, A. Miller, S. Chen, B. Williams, E. Theodorou and T. Jacks, 2000. Targeted disruption of the three Rb-related genes leads to loss of G(1) control and immortalization. Genes development, 14 (23): 3037-3050.

Sargeant, I.R., L.A. Loizou, J.S. Tobias, G. Blackman, S. Thorpe and S.G. Bown, 1992. Radiation enhancement of laser palliation for malignant dysphagia: a pilot study. Gut, 33 (12): 1597-1601.

Schultz, L.B., N.H. Chehab, A. Malikzay and T.D. Halazonetis, 2000. p53 binding protein 1 (53BP1) is an early participant in the cellular response to DNA double-strand breaks. J. Cell Biol., 151 (7): 1381-1390.

Shackelford, R.E., W.K. Kaufmann and R.S. Paules, 1999. Cell cycle control, checkpoint mechanisms, and genotoxic stress. Environ. Health Perspect., 107 Suppl 1: 5-24.

Shelton, D.N., E. Chang, P.S. Whittier, D. Choi and W.D. Funk, 1999. Microarray analysis of replicative senescence. Current biology, 9 (17): 939-945.

Sibanda, B.L., S.E. Critchlow, J. Begun, X.Y. Pei, S.P. Jackson, T.L. Blundell and L. Pellegrini, 2001. Crystal structure of an Xrcc4-DNA ligase IV complex. Nat. Struct. Biol., 8 (12): 1015-1019.

Smider, V., W.K. Rathmell, G. Brown, S. Lewis and G. Chu, 1998. Failure of hairpin-ended and nicked DNA To activate DNA-dependent protein kinase: implications for V(D)J recombination. Mol. Cell. Biol., 18 (11): 6853-6858.

Song, Q., S.P. Lees Miller, S. Kumar, Z. Zhang, D.W. Chan, G.C. Smith, S.P. Jackson, E.S. Alnemri, G. Litwack, K.K. Khanna and M.F. Lavin, 1996. DNA-dependent protein kinase catalytic subunit: a target for an ICE-like protease in apoptosis. EMBO J., 15 (13): 3238-3246.

Stewart, G., B. Wang, C. Bignell, A.M.R. Taylor and S. Elledge, 2003. MDC1 is a mediator of the mammalian DNA damage checkpoint. Nature, 421 (6926): 961-966.

Stuckey, J.A. and J.E. Dixon, 1999. Crystal structure of a phospholipase D family member. Nat. Struct. Biol., 6 (3): 278-284.

Suh, D., D.M. Wilson and L.F. Povirk, 1997. 3'-phosphodiesterase activity of human apurinic/apyrimidinic endonuclease at DNA double-strand break ends. Nucleic Acids Res., 25 (12): 2495-2500.

Sung, P. and H. Klein, 2006. Mechanism of homologous recombination: mediators and helicases take on regulatory functions. Nature reviews.Molecular cell biology, 7 (10): 739-750.

Takashima, H., C. Boerkoel, J. John, G. Saifi, M.A.M. Salih, D. Armstrong, Y. Mao, F. Quiocho, B. Roa, M. Nakagawa, D. Stockton and J. Lupski, 2002. Mutation of TDP1, encoding a topoisomerase I-dependent DNA damage repair enzyme, in spinocerebellar ataxia with axonal neuropathy. Nat. Genet., 32 (2): 267-272.

Takata, M., M.S. Sasaki, E. Sonoda, C. Morrison, M. Hashimoto, H. Utsumi, Y. Yamaguchi Iwai, A. Shinohara and S. Takeda, 1998. Homologous recombination and non-homologous end-joining pathways of DNA double-strand break repair have overlapping roles in the maintenance of chromosomal integrity in vertebrate cells. EMBO J., 17 (18): 5497-5508.

Todaro, G.J. and H. Green, 1963. Quantitative studies of the growth of mouse embryo cells in culture and their development into established lines. J. Cell Biol., 17: 299-313.

Tuteja, N., R. Tuteja, A. Ochem, P. Taneja, N.W. Huang, A. Simoncsits, S. Susic, K. Rahman, L. Marusic and J. Chen, 1994. Human DNA helicase II: a novel DNA unwinding enzyme identified as the Ku autoantigen. EMBO J., 13 (20): 4991-5001.

Valerie, K. and L. Povirk, 2003. Regulation and mechanisms of mammalian double-strand break repair. Oncogene, 22 (37): 5792-5812.

Walker, J.R., R.A. Corpina and J. Goldberg, 2001. Structure of the Ku heterodimer bound to DNA and its implications for double-strand break repair. Nature, 412 (6847): 607-614.

Wang, S., M. Guo, H. Ouyang, X. Li, C. Cordon Cardo, A. Kurimasa, D.J. Chen, Z. Fuks, C.C. Ling and G.C. Li, 2000. The catalytic subunit of DNA-dependent protein kinase selectively regulates p53-dependent apoptosis but not cell-cycle arrest. Proc. Natl. Acad. Sci. U. S. A., 97 (4): 1584-1588.

Wang, Y., D. Cortez, P. Yazdi, N. Neff, S.J. Elledge and J. Qin, 2000. BASC, a super complex of BRCA1-associated proteins involved in the recognition and repair of aberrant DNA structures. Genes development, 14 (8): 927-939.

Ward, J.F., 1990. The yield of DNA double-strand breaks produced intracellularly by ionizing radiation: a review. Int. J. Radiat. Biol., 57 (6): 1141-1150.

Ward, J.F., 1988. DNA damage produced by ionizing radiation in mammalian cells: identities, mechanisms of formation, and reparability. Prog. Nucleic Acid Res. Mol. Biol., 35: 95-125.

Watson, J.D. and F.H. Crick, 1953. Genetical implications of the structure of deoxyribonucleic acid. Nature, 171 (4361): 964-967.

West, R.B., M. Yaneva and M.R. Lieber, 1998. Productive and nonproductive complexes of Ku and DNA-dependent protein kinase at DNA termini. Mol. Cell. Biol., 18 (10): 5908-5920.

Weterings, E. and D. Chen, 2007. DNA-dependent protein kinase in nonhomologous end joining: a lock with multiple keys?. J. Cell Biol., 179 (2): 183-186.

Whitmore, G.F., A.J. Varghese and S. Gulyas, 1989. Cell cycle responses of two X-ray sensitive mutants defective in DNA repair. Int. J. Radiat. Biol., 56 (5): 657-665.

Wilson, D.S., A.D. Keefe and J.W. Szostak, 2001. The use of mRNA display to select high-affinity protein-binding peptides. Proceedings of the National Academy of Sciences, 98 (7): 3750-3755.

Woo, R.A., K.G. McLure, S.P. Lees Miller, D.E. Rancourt and P.W. Lee, 1998. DNA-dependent protein kinase acts upstream of p53 in response to DNA damage. Nature, 394 (6694): 700-704.

Wright, W.E. and J.W. Shay, 2000. Telomere dynamics in cancer progression and prevention: fundamental differences in human and mouse telomere biology. Nat. Med., 6 (8): 849-851.

Wu, X. and M.R. Lieber, 1996. Protein-protein and protein-DNA interaction regions within the DNA end-binding protein Ku70-Ku86. Mol. Cell. Biol., 16 (9): 5186-5193.

Xiao, Z., Z. Chen, A. Gunasekera, T. Sowin, S. Rosenberg, S. Fesik and H. Zhang, 2003. Chk1 mediates S and G2 arrests through Cdc25A degradation in response to DNA-damaging agents. J. Biol. Chem., 278 (24): 21767-21773.

Yoo, S. and W.S. Dynan, 1999. Geometry of a complex formed by double strand break repair proteins at a single DNA end: recruitment of DNA-PKcs induces inward translocation of Ku protein. Nucleic Acids Res., 27 (24): 4679-4686.

Zhang, Y., T. Hunter and R. Abraham, 2006. Turning the replication checkpoint on and off. Cell cycle, 5 (2): 125-128.

Zhou, T., K. Akopiants, S. Mohapatra, P. Lin, K. Valerie, D.A. Ramsden, S.P. Lees-Miller and L.F. Povirk, 2009. Tyrosyl-DNA phosphodiesterase and the repair of 3′-phosphoglycolate-terminated DNA double-strand breaks. DNA Repair, 8 (8): 901-911.

Zhou, T., K. Akopiants, S. Mohapatra, P. Lin, K. Valerie, D.A. Ramsden, S.P. Lees-Miller and L.F. Povirk, 2009. Tyrosyl-DNA phosphodiesterase and the repair of 3′-phosphoglycolate-terminated DNA double-strand breaks. DNA Repair, 8 (8): 901-911.

Zhou, T., J. Lee, H. Tatavarthi, J. Lupski, K. Valerie and L. Povirk, 2005. Deficiency in 3'-phosphoglycolate processing in human cells with a hereditary mutation in tyrosyl-DNA phosphodiesterase (TDP1). Nucleic Acids Res., 33 (1): 289-297.

VITA

Tong Zhou was born on August 10, 1965 in Anshan, Liaoning province, China. She graduated with a Bachelor's degree in Clinical Medicine from China Medical University, Shenyang, China in 1989. She worked in Shenyang Medical College Hospital, Shenyang, China as a physician in the Department of Obstetrics and Gynecology from 1989 to 1994, and became an attending physician from 1994 to 2000. She joined Dr. Povirk's laboratory as a postdoctoral research associate from 2001 to 2007, and later on, was appointed as a lab specialist. She joined the Masters program in Molecular Biology and Genetics in 2009.